NACA

RESEARCH MEMORANDUM

PERFORMANCE OF A RAM-JET-TYPE COMBUSTOR WITH FLAME HOLDERS IMMERSED IN THE COMBUSTION ZONE

By Roland Breitwieser

Lewis Flight Propulsion Laboratory
Cleveland, Ohio

NATIONAL ADVISORY COMMITTEE FOR AERONAUTICS

WASHINGTON
November 1, 1948

Classification cancelled (or changed to Unclassified)

By Authority of NASA Tech Pub Announcement #101
(OFFICER AUTHORIZED TO CHANGE)

By ..... 25 May 56
NAME AND

NK
GRADE OF OFFICER MAKING CHANGE)

6 April 61
DATE

NACA RM No. E8F21

NATIONAL ADVISORY COMMITTEE FOR AERONAUTICS

RESEARCH MEMORANDUM

PERFORMANCE OF A RAM-JET-TYPE COMBUSTOR WITH FLAME HOLDERS IMMERSED IN THE COMBUSTION ZONE

By Roland Breitwieser

SUMMARY

The beneficial effects on stability limits and combustion efficiency produced by the application of surfaces immersed in the combustion zone to a ram-jet-type burner are reported. The flame holders, which are representative of the conventional-type ram-jet flame holders, consisted of a single row of aluminum-sprayed carbon wedges. For the configurations introducing flame holders in the combustion zone, additional rows of the same type of carbon wedge were introduced downstream of the first row of wedges. Investigations were made with one, two, three, and four rows of wedges at simulated sea-level and altitude subsonic ram-jet flight conditions. The use of standard refractory forms in attaining surface combustion was also investigated.

The addition of rows of wedges immersed in the combustion zone regularly extended the stability limits of combustion. The maximum allowable inlet-air velocity for stable combustion with the four-row configuration was approximately twice the maximum allowable inlet-air velocity with the conventional single-row configuration at the penalty of only a slight additional total-pressure loss across the burner. Heat-release rates as high as 50,000,000 Btu per cubic foot per hour per atmosphere were attained with the four-row configuration. The combustion efficiency was aided by the addition of immersed surfaces in the combustion zone.

INTRODUCTION

An important problem in the broad field of combustion and its application to various engine cycles is to maintain stable and efficient combustion with low-drag combustors at high heat-release rates. The phenomenon of surface combustion and its coincident high reaction rates is well known (reference 1); however, the process normally involves high pressure losses, which prohibit the conventional use of surface combustion in a ram-jet combustor.

The application of the process of combustion on hot surfaces in the initial phase of stabilization of combustion in a ram-jet-engine cycle was investigated at the NACA Cleveland laboratory and is reported herein. The technique examined was that of using heat-resistant flame holders immersed in the combustion zone of the experimental combustion chamber.

A preliminary investigation, which is reported in the appendix, included various types and designs of refractories that were made to determine a suitable material and configuration for a flame holder. The flame holder selected was a wedge-shaped block of graphite, which had been spray-coated with aluminum. Two such wedges placed parallel across the cross section of the combustion chamber represented a conventional ram-jet-type flame holder. Additional rows of similar wedges were introduced downstream of the original row to evaluate the effect of surfaces immersed in the flame zone. No attempt was made to determine an optimum configuration or material for ram-jet flame holders but rather the relative improvement to be gained by applying an old technique to a new field.

Data were determined for the stability limits of combustion, combustion efficiency, heat-release rates, and pressure losses at two inlet-air conditions to compare the performance of the combustor incorporating a conventional single-row flame holder with the performance of the combustor incorporating additional rows of flame holders in the combustion zone. Configurations of one, two, three, and four rows of flame holders were investigated. A study was also made of the effect on pressure fluctuations and combustion stability of addition of water in the form of a fine spray at the combustion-chamber outlet.

APPARATUS

The combustion air was supplied to the combustion-air system (fig. 1) by the central laboratory supply. The inlet-air temperature was automatically controlled by an electric preheater and bypass unit upstream of the air-metering orifice. The inlet-air temperature was indicated by a thermocouple shielded from the flame zone. The orifice pressure was maintained constant and the flow rate was regulated by a sleeve valve downstream of the orifice. The critical pressure ratio across the regulating valve was always exceeded in order to maintain sonic velocity at the valve and thereby minimizing pressure disturbances in the inlet duct. The combustion-chamber pressure was regulated by an exhaust valve and bypass leading to atmospheric exhaust.

The burner layout is shown in figure 2. Propane, which was supplied from the laboratory fuel system, was measured by an orifice installation and introduced into the burner through a movable fuel distributor as shown in section A-A of figure 2. The point of entry

of the propane was kept a constant distance (10 in.) upstream of the nearest row of flame holders, which established an equal fuel-air mixing length for the various trials.

The flame holders were graphite wedges sprayed with aluminum and mounted across a removable section of the 5-inch-diameter burner duct, which was held in place by a split sleeve. This sleeve assembly was enclosed in a pressurized chamber through which cooling air was introduced by jets impinging on the wedge flame-holder assembly. The cooling-air flow was measured by an orifice installation. The outlet of the pressurized chamber was connected to the burner exhaust so that only a slight differential pressure existed across the flame-holder mounting sleeve; the low differential pressure minimized leakage of cooling air into the flame-holder system.

Two wedges constituting 28-percent total obstructed area symmetrically mounted 3 inches apart comprised each row and are shown in section B-B of figure 2. The wedge holder is illustrated in figure 3, which shows one row of wedges in place ready for introduction into the combustion chamber. Wedges were added upstream of the rear row of wedges to form the multiple-row configurations. The location of the wedges for the various configurations is shown in figure 4.

A nominal 10-inch combustion-chamber length was maintained constant by placing a water spray bar 10 inches downstream of the rear of the upstream wedges. The water spray bar (section C-C of fig. 2) consisted of a main supply tube from which smaller tubes extended radially. The water was sprayed normal to the exhaust stream from numerous holes in the tubes. The walls of the combustion chamber downstream of the wedge holder were cooled by a water jacket. The mass flow rates of water to the jacket and the spray were measured by orifices. The rate of water flow to the spray was maintained at a sufficiently high value to reduce pressure fluctuations in the gas flow to a sufficiently low value for satisfactory operation, as will be subsequently discussed.

The pressure loss across the burner section was determined by readings obtained from wall static taps 3 inches upstream of the removable burner section and 6 inches downstream of the downstream row of wedges.

The thermocouple rakes (section D-D of fig. 2), which consisted of 12 chromel-alumel thermocouples located at centers of equal areas, were mounted 11 feet downstream of the rear wedge row in an 8-inch-diameter section. Total-pressure rakes were initially installed at the thermocouple station, but preliminary experiments indicated a substantially constant-velocity profile for the range of values to be used and the pressure rakes were removed.

[redacted]

PROCEDURE

Determination of Stability-Limit Data

Two combinations of inlet-air pressure and temperature were used to determine the stable operating limits of the combustor configurations. One combination corresponded to a flight Mach number of 1.0 at sea level and 100-percent diffuser efficiency for a hypothetical ram jet, namely, an inlet-air pressure of 55 inches of mercury absolute and an inlet-air temperature of 160° F. The other combination corresponded to a flight Mach number of 1.0 at an altitude of 10,000 feet and 100-percent diffuser efficiency, namely, an inlet-air pressure of 40 inches of mercury absolute and an inlet-air temperature of 120° F. A water spray rate of 0.67 pound per second was maintained for both operating conditions.

Stability-limit data were taken by varying fuel-air ratio and inlet-air velocity to the bounds of stable combustion with spark on; the stability limit was noted and the stable operating range reentered. The tentative stability limit was then approached with spark off, the inlet conditions were held constant for a length of time sufficient to insure constant inlet conditions, and the new stability-limit point recorded. The stability-limits were visually verified by an axial view through the burner-inlet elbow and by observation of the static-pressure loss across the burner. Stability limit was defined as a point where burning ceased to be homogeneous across the burner cross section and was characterised by an abrupt reduction of static-pressure loss. When deviations of the check data from the existing data were noted, the wedge holder was removed to inspect for missing or deteriorated wedges.

Determination of Combustion Efficiency

The combustion-efficiency data were determined at an inlet-air pressure of 55 inches of mercury absolute and an inlet-air temperature of 160° F, which corresponded to the simulated sea-level operating conditions.

Data were only determined for the combustor configurations with a single row and with four rows of wedges. The efficiency data for the single row of wedges were taken after establishing the operating range from the stability-limit data. The fuel-air ratio was varied and data were taken at two inlet-air velocities within the operating range; data were also taken for various inlet-air velocities at the fuel-air ratio at which the maximum permissible inlet-air velocity

had occurred. The investigation of efficiency with the four-row configuration was limited to runs at various inlet-air velocities for a fuel-air ratio of approximately 0.0525, because of the short life of the immersed wedges.

Combustion efficiency was determined by a heat-balance method similar to the method outlined in reference 2. The sum of the enthalpy changes of the fuel-air mixture, the spray water, the cooling air, and the cooling water were divided by the input energy of the fuel. The thermodynamic data of the properties of the aforementioned substances were obtained from references 3 to 6. The rate of water flow to the spray was regulated to keep the outlet-gas temperature at a sufficiently high value to insure complete vaporization of the water spray.

Pressure Fluctuations

A series of runs was conducted to establish the effect of the water spray on burner characteristics. The single-row configuration was used for the investigation at simulated sea-level inlet-air conditions and an inlet-air velocity of 115 feet per second. For eight water flow rates, the lean limit fuel-air ratio was recorded. Burner pressure-time oscillograph traces from a capacity-type pressure pickup were photographed in a similar investigation for operation at various water-spray rates. In the pressure-time investigation, the fuel-air ratio was held constant at a value of 0.06, which is slightly richer than the lean-limit blow-out. The water flow rate was varied and pressure traces photographed at time intervals of 1/25, 1/5, and 1 second.

Determination of Pressure Losses

The inlet-air dynamic pressures were calculated from the air mass flows, average inlet-air temperatures, and average inlet-air static pressures. Experimental momentum-pressure losses were found by subtracting the measured isothermal (friction) pressure loss from the measured pressure loss during burning for the same inlet-air conditions. Theoretical momentum-pressure losses were computed by the simultaneous solution of the momentum and continuity equations using the inlet Mach number and temperature ratio across the burner. The combustion chamber was assumed to be of a constant cross section.

[redacted]

RESULTS AND DISCUSSIONS

Stability Limits

The effect on the stability limit of the addition of rows of wedges in the combustion zone is shown in figure 5 for the simulated 10,000-foot-altitude operating conditions of inlet-air pressure and temperature of 40 inches of mercury absolute and 120° F, respectively. The stability limit of the single-row configuration, which essentially constituted a conventional flame holder, is shown in figure 5(a). The maximum allowable inlet-air velocity for the single-row unit was 93 feet per second and the range of stable operation was confined to fuel-air ratios above 0.064. There was a minimum inlet-air-velocity stability limit as well as a maximum inlet-air-velocity stability limit as evidenced by the lower branch of the curve in figure 5(a). A stability limit due to flash back (that is, propagation of the flame into the zone upstream of the flame holders) occurred below an inlet-air velocity of 83 feet per second at lean mixtures. The inlet-air velocity at this stability limit decreased with increases in fuel-air ratio. When flash back occurred, the flame was no longer stabilized on the wedge flame holders but oscillated between the flame holders and the point of fuel introduction.

The addition of a row of wedges in the combustion zone, which gave a two-row configuration, increased the maximum inlet-air velocity to 112 feet per second (fig. 5(b)). The three-row configuration gave a maximum allowable inlet-air velocity of 136 feet per second (fig. 5(c)). The four-row unit gave a maximum inlet-air velocity of 193 feet per second (fig. 5(d)), which is more than twice the maximum inlet-air velocity of the single-row configuration. The insertion of each additional row of wedges increased the stable operation range of fuel-air ratios as well as the range of inlet-air velocities. The curves of figures 5(a) to 5(d) are superimposed for comparison in figure 5(e). The maximum inlet-air velocity occurred at progressively leaner fuel-air ratios as the number of rows of wedges was increased. The maximum inlet-air velocity for each configuration is plotted against the number of rows of wedges in figure 5(f).

Data for the same configurations but at the operating condition of inlet-air pressure and temperature of 55 inches mercury absolute and 160° F, respectively,are shown in figure 6. Increasing the inlet-air pressure from 40 to 55 inches of mercury absolute and increasing the inlet-air temperature from 120° to 160° F for a burner consisting of a single row of wedges increased the maximum inlet-air velocity from 93 to 170 feet per second (figs. 5(a) and 6(a)), respectively.

The maximum inlet-air velocities at the simulated sea-level conditions were 170 feet per second for the single row (fig. 6(a)), 190 for the two rows (fig. 6(b)), 194 for the three rows (fig. 6(c)), and 292 for the four rows of wedges (fig. 6(d)) as shown on the stability-limit curves. The stability-limit data for the four-row configuration are incomplete, inasmuch as the laboratory propane supply was inadequate for the high mass-flow runs. The composite results of the stability-limit investigation at the simulated sea-level inlet-air condition are shown in figure 6(e); the general trends were the same as at the simulated-altitude condition. The addition of each row of wedges increased the range of fuel-air ratio as well as the range of inlet-air velocity. The maximum inlet-air velocity for each configuration plotted against the number of rows of wedges is shown in figure 6(f). The value of 292 feet per second for four rows of wedges is the maximum observed value but not necessarily the maximum permissible value.

In attaining the data for the immersed-wedge configurations, operation at relatively low velocities in the stable band of operation was necessary in order to heat the immersed wedges. After the immersed surfaces attained relatively high temperatures, stabilization of combustion at the higher inlet-air velocities was possible.

The check points shown in figures 6(a), 6(b), and 6(d) illustrate the accurate reproducibility of the stability-limit data.

Combustion Efficiency

The burning zone in this investigation was, in all cases, confined to a length of 10 inches from the upstream flame holder to the quenching water sprays. The effect of inlet-air velocity on combustion efficiency at simulated sea-level inlet-air conditions for the single-row configuration at a fuel-air ratio of 0.06 is shown in figure 7. Included on the curve are the stability limits taken from figure 6(a). An increase of inlet-air velocity from 96 feet per second to 170 feet per second decreased the combustion efficiency from 67 to 52 percent, which is a relative decrease of 20 percent within the stability range.

The combustion efficiency at a constant inlet-air velocity of 115 feet per second for various fuel-air ratios in the stable operation range is shown in figure 8(a). The data indicate maximum combustion efficiency of 65 percent in the lean portion of the stable-operation range. At an inlet-air velocity of 155 feet per second (fig. 8(b)), no appreciable change in efficiency (constant at approximately 62 percent) is evident for the fuel-air-ratio range in the

stable-combustion region. The values of combustion efficiency rapidly decreased (a relative change of 30 to 40 percent) at the stability limits, which is coincident with the sudden change in the combustion-chamber pressure and cessation of burning noted during the stability-limit investigation at similar conditions. The rapid change of combustion efficiency at the stability limits constitutes a further check of the stability-limit data.

The combustion-efficiency investigation of the configuration consisting of four rows of wedges was difficult to obtain because of the short life of the immersed wedges at the high heat-release rates and also because of the difficulty in maintaining the operating variables at the desired values. The average combustion efficiency of the four-row configuration at an inlet-air pressure varying from 38 to 60 inches of mercury absolute, inlet-air temperature of 160° F, fuel-air ratio of 0.0505 to 0.0550, and a constant inlet-air velocity of 210 feet per second is shown in figure 9(a). The combustion efficiency increased from 33 percent at an inlet-air pressure of 39 inches of mercury absolute to 74 percent at an inlet-air pressure of 60 inches of mercury absolute. The increase in combustion efficiency with increase in inlet-air pressure produced serious pressure-control problems; the control of the combustion-chamber pressure was further aggrevated by an approach to thermal choking at the high inlet-air velocities. The time required to stabilize inlet conditions and to record data necessary for efficiency determinations was of the order of magnitude of the life of the immersed wedges. Wedges were replaced as many as three or four times when operating at conditions that gave high heat-release rates before reliable data could be recorded. The curve of efficiency against inlet-air velocity shown in figure 9(b) at best expresses the average efficiency of a range of values because of the difficulty in setting and stabilizing the inlet conditions. As a result, the efficiency data are shown as variable by arrows on the data points. The location of the arrow points approximate the degree of uncertainty in the values of efficiency. The data indicate that for a configuration consisting of four rows of wedges the efficiency is about 58 percent at the simulated sea-level conditions and is not appreciably affected by a change in inlet-air velocity.

Heat-Release Rates

Heat-release rates as high as 50,000,000 Btu per cubic foot of burner volume per hour per atmosphere were observed at an inlet-air pressure of 60 inches of mercury and at an inlet-air velocity of 210 feet per second for the four-row configuration. The heat-liberation rate was about 40,000,000 Btu per cubic foot of burner

volume per hour per atmosphere at the highest inlet-air-velocity point shown in figure 9(b). The nominal combustor length was 10 inches and the combustion reaction was assumed quenched at the plane of the water sprays in estimating the reaction rates.

Effect of Water Flow to Quench Spray

The effect on the stability limit of changing the rate of water flow to the quenching spray is shown in figure 10. The inlet-air conditions corresponded to the lean-stability limit of the single-row-wedge configuration at an inlet-air pressure of 55 inches of mercury absolute and an inlet-air temperature of 160° F. The rate of water flow to the spray was varied from 30 to 120 percent of the value held constant in obtaining the stability-limit data. Decreasing the rate of flow to the water spray while maintaining all other operating conditions constant gave a lean limit of stable combustion at progressively higher fuel-air ratios. The change in the stability limit in terms of fuel-air ratio with change in flow rates to the spray was relatively insensitive near the value used in the stability-limit investigation; however, as the flow was reduced to approximately one-third of the value used in the stability-limit investigation, the combustion became exceedingly rough and difficult to define, as can be seen from figure 10. The spray ceased to be homogeneous at very low flow rates and did not cover the entire cross section of the burner duct.

Photographs of the pressure-time curves obtained from the combustion chamber with a condenser-type pickup in conjunction with a cathode-ray oscillograph for various rates of water flow are shown in figure 11. Each vertical unit of the superimposed gridwork represents a pressure of 0.5 pound per square inch and each horizontal unit represents a time interval of 1/200 second. Photographs at the four rates of water flow were taken at three exposure times; at the 1/25-second exposure time, a single pressure trace was recorded; whereas at longer exposure times, a cumulative series of traces was recorded, which showed the occasional high-pressure disturbances. At the flow rates to the quenching spray in the range of values used in the stability-limit data, the amplitude of the pressure change was in the order of 1 to 2 pounds per square inch. As the rate of flow to the quenching spray was decreased, the amplitude of the pressure disturbances increased. At a flow rate of 0.10 pound of water per second to the quenching spray, which is about 1/7 of the rate of flow for the stability-limit investigation, the pressure fluctuations were as high as 12 pounds per square inch or about 50 percent of the burner static pressure. At the low-flow conditions, the combustion was unstable

and necessitated operation with spark on. The frequency of the characteristic wave at rates of water flow to the spray of 0.60 and 0.80 pound per second was about 40 cycles per second and decreased to an estimated 20 cycles per second at the low flow rates to the spray. The frequency of 40 cycles per second is equivalent to the computed frequency of the reflection wave from the end of the combustion zone to the inlet-air valve, that is, the time interval for sound to travel twice the distance between inlet valve and combustion chamber at observed inlet-air condition. Critical pressure ratios were always exceeded across the inlet-air control valve. A high rate of water flow to the quenching spray, which corresponded to values for more homogeneous mixing of exhaust gases and quenching water, appeared to damp out the pressure disturbances of the experimental burner unit.

The efficiency determinations at the simulated altitude conditions were not investigated because of the low rates of water spray flow required to insure vaporization of the spray at the low heat-release rates. The low rates of water flow introduced severe pressure oscillations, which disguised the results of the efficiency investigation.

Pressure Losses

The isothermal-pressure losses (no combustion) for the various configurations expressed in terms of the static-pressure loss Δp divided by the inlet dynamic pressure q are shown in figure 12. The value of $\Delta p/q$ had an average value of 0.68 for the single row of wedges at simulated altitude conditions and increased about 7 percent (average) for each row of wedges added downstream. The value of $\Delta p/q$ obtained at simulated sea-level conditions was about 0.74 and again increased about 7 percent (average) for each row of wedges added as the simulated altitude data. The absolute values for $\Delta p/q$ in the isothermal investigations were low and fabrication limitations prevented installation of special static-pressure taps necessary for a more accurate correlation.

The ratio of the actual momentum-pressure loss to the computed momentum-pressure loss (static Δp) for the burning condition is plotted against the computed pressure loss for both the one- and four-row configurations in figure 13. The actual momentum-pressure loss was roughly approximated by assuming the momentum-pressure loss equal to the observed total-pressure drop minus the equivalent isothermal-pressure loss at the same inlet conditions. The pressure-drop

ratio for the four-row configuration appears to be slightly higher than that for the single-row configuration indicating slightly higher pressure losses for the immersed configuration. The data as presented are somewhat inconclusive but show that the relative magnitude of the pressure-drop ratio for both configurations is of the same order.

Durability of Flame Holders

The life of the graphite wedges varied with the operating conditions. The immersed wedges had a life expectancy in excess of 30 minutes at the lower heat-release rates. Lean fuel-air ratios and high heat-release rates both had adverse effects on the life of the submerged wedges. The life of the wedges was approximately 10 minutes at the most severe conditions encountered in this investigation. Wedges in various stages of deterioration are shown in figure 14. The wedge farthest to the right was a new unit and the wedges to the left were subjected to increasingly severe operation. Failure of the wedges occurred by erosion of the protective coat of aluminum oxide followed by oxidation of the graphite body. A protective plating of rhodium on the graphite body prior to the aluminum spray lengthened the life of the wedge but not sufficiently to warrant the additional fabrication problem. In no case was there evidence of failure of the graphite wedges by heat shock.

SUMMARY OF RESULTS

From a performance investigation of a ram-jet-type combustor with flame holders immersed in the combustion zone, the following results were obtained:

Primary Investigation

1. The stepwise addition of rows of wedges immersed in the combustion zone regularly extended the stability limit. The maximum allowable inlet-air velocity for the four-row immersed-wedge configuration was about twice the maximum allowable inlet-air velocity for the conventional single-row configuration at the two inlet-air conditions investigated.

2. The efficiency of the four-row immersed-wedge flame holder appeared to be independent of inlet-air velocity for the range investigated.

3. Increasing the inlet-air velocity from 96 to 170 feet per second showed a relative decrease of the combustion efficiency of about 20 percent for the single-row configuration.

4. Combustion efficiency of the four-row configuration increased rapidly with an increase in pressure.

5. Heat-release rates as high as 50,000,000 Btu per cubic foot per hour per atmosphere were attained with the four-row configuration.

6. The ratio of the isothermal total-pressure loss to the inlet dynamic pressure was 0.68 at the simulated altitude condition and was 0.74 at the simulated sea-level condition for the single-row configuration and increased about 7 percent (average) for each row added downstream.

7. Wedges composed of graphite with a protective coating attained life sufficient for short-duration runs of 10 to 20 minutes.

8. Severe pressure oscillations may build up in a closed-duct burner unit. Water that was sprayed in the combustion zone to determine combustor lengths damped the pressure waves that were caused by the resonant characteristics of the combustion-air system.

Preliminary Investigation

Standard ceramics incorporated into burner flame holders exhibited little resistance to thermal shock but did exhibit positive flame-holding properties.

Lewis Flight Propulsion Laboratory,
National Advisory Committee for Aeronautics,
Cleveland, Ohio.

APPENDIX - PRELIMINARY INVESTIGATION

A number of ceramic flame holders were examined for flame-holding characteristics at high heat-release rates. The combustion inlet-air and exhaust systems were the same as shown for the immersed-wedge investigation (fig. 1). The inlet-air pressure was measured by a static wall tap upstream of the combustion zone.

The ceramic-refractory flame-holder configurations investigated were held by a 5-inch replaceable sleeve, as shown in the schematic combustion-chamber layout (fig. 15). The combustion air was divided into primary air leading to the flame holder and secondary air, which was used as an exhaust-gas diluent. As shown in figure 15, the primary air flow was measured by an orifice installation. The fuel was sprayed into the combustion chamber with a hollow-cone spray nozzle (rated at 2 gal/hr at 100 lb/sq in.) located as shown in figure 15. Twelve chromel-alumel thermocouples, which were used to measure outlet-gas temperatures were spaced at centers of equal areas and were located 11 feet downstream of the burner section.

Methods

The short life of the refractory configurations necessitated an abbreviated procedure.

The combustion-chamber pressure was held constant at 1 atmosphere and the inlet-air temperature varied from 100° to 200° F. The fuel was 62-octane gasoline. The fuel-air ratio varied between 0.05 and 0.067.

The primary inlet-air velocity was increased to the limit for stable combustion and this limiting velocity and all other pertinent data were recorded. Combustion efficiencies were measured at velocities just below the limit velocity for stable combustion. Sufficient air was proportioned through the secondary-air passages to reduce the outlet-gas temperature and thus to prevent failure of downstream instrumentation.

Results and Discussion

The ceramic-refractory investigations were hampered by repeated failures of the materials because of thermal shock. A series of trial burner units are illustrated in figure 16. In general, the

units as shown were constructed from standard ceramic forms, inasmuch as special configurations involved high material costs and a long time delay in fabrication.

A combustion chamber consisting of 3-inch lengths of 1/2-inch-inside-diameter, 1/8-inch-wall porous aluminum-oxide tubes clustered (fig. 16(a)) burned at inlet-air velocities (based on open area in the tube bank) up to 50 feet per second and gave a combustion efficiency of 60 percent. The tubes failed from thermal shock. A similar configuration with 1/2-inch-inside-diameter, 1/8-inch-wall tubes composed of an impervious metallic oxide ceramic with a glazed surface was next tried (fig. 16(b)) but the smooth impervious surface prevented stabilization of combustion. The configuration shown in figure 16(a) was doubled in length to 6 inches as shown in figure 16(c). Increasing the length of the porous aluminum oxide stabilized combustion at an inlet-air velocity of 100 feet per second based on open area through the tube bank and gave a combustion efficiency of 80 percent. The tubes then failed from heat shock. The unit composed of the glazed ceramic was increased in length to 12 inches as shown in figure 16(d) and the glazed surface again failed to sustain combustion.

Burners consisting of multiple rows of ceramic tubes shown in figures 16(e) and 16(f) were next investigated. The burner shown in figure 16(e) consisted of two separate banks or clusters of tubes; the first cluster was composed of 1/2-inch-inside-diameter, 1/8-inch-wall porous aluminum-oxide tubes 2 inches long and was followed by another cluster composed of 1/2-inch-inside-diameter, 1/8-inch-wall glazed ceramic tubes 3 inches long. The limiting inlet-air velocity based on open area through the tube bank was 74 feet per second and combustion efficiency was 85 percent. These performance values may not be true performance limitations, inasmuch as the units failed from thermal shock before completion of the investigation. The burner composed of three rows of clusters of 1/4-inch-inside-diameter, 1/16-inch-wall glazed ceramic tubes, each $1\frac{1}{2}$-inches long (fig. 16(f)), allowed stable combustion to a velocity based on open area through the tube bank of 90 feet per second before thermal failure prevented completion of the investigation. The combustion performance appeared to be better for the additive units as compared to the single-cluster configurations of the same total tube length.

A ceramic impregnated screen (fig. 16(g)) was constructed primarily to achieve maximum surface with a minimum of blocked area but failed because of breakdown of the ceramic coating before data could be recorded.

[redacted]

Tandem aluminum-oxide cones (fig. 16(h)) exhibited fair stability but gave low efficiency and failed as a result of heat shock.

The impingement of liquid fuel particles from the spray on the ceramics appeared to increase the severity of the thermal-shock problem. Propane was therefore substituted as a fuel in the investigation of the configuration shown in figure 16(i). The configuration consisted of a series of metal gutters followed by a gridwork of metal plates, which were all mounted in a ceramic shell. Sheet tungsten used in the fabrication of the gutters and gridwork was plated with a protective coating of rhodium. At an inlet-air pressure and temperature of 55 inches of mercury absolute and 160° F, respectively, the burner unit failed from rupture of the gutters by pressure fluctuations and destruction of the ceramic housing by heat shock. The maximum inlet-air velocity based on burner diameter was 200 feet per second.

The ceramic configurations exhibited little resistance to thermal shock, which prevented the attainment of exact data. However, the immersed surfaces, that is, surfaces introduced behind the upstream flame holder, exhibited positive flame-holding properties. The burner configuration that incorporated a series of gutters (fig. 16(i)) in the combustion region gave the best combustion performance in addition to offering ease of fabrication. The flame holder composed of graphite wedges sprayed with aluminum oxide was evolved from the tungsten-gutter configuration. The stepwise addition of the wedge-type flame-holding surfaces in the combustion zone is discussed in the main text of the report.

REFERENCES

1. Bone, W. A., and Townsend, Donald T. A.: Flame and Combustion in Gases. Longman's Greene & Co., Ltd. (London), 1927, pp. 30-32, 461-472.

2. Cervenka, A. J., and Miller, R. C.: Effect of Inlet-Air Parameters on Combustion Limit and Flame Length in 8-Inch-Diameter Ram-Jet Combustion Chamber. NACA RM No. E8C09, 1948.

3. Keenan, Joseph H., and Kaye, Joseph: Thermodynamic Properties of Air. John Wiley & Sons, Inc., 1945, pp. 5-20.

4. Keenan, Joseph H., and Keyes, Frederick G.: Thermodynamic Properties of Steam. John Wiley & Sons, Inc., 1936, pp. 28-30, 40-41.

[redacted]

5. Pinkel, Benjamin, and Turner, L. Richard: Thermodynamic Data for the Computation of the Performance of Exhaust-Gas Turbines. NACA ARR No. 4B25, 1944.

6. Turner, L. Richard, and Lord, Albert M.: Thermodynamic Charts for the Computation of Combustion and Mixture Temperatures at Constant Pressure. NACA TN No. 1086, 1946.

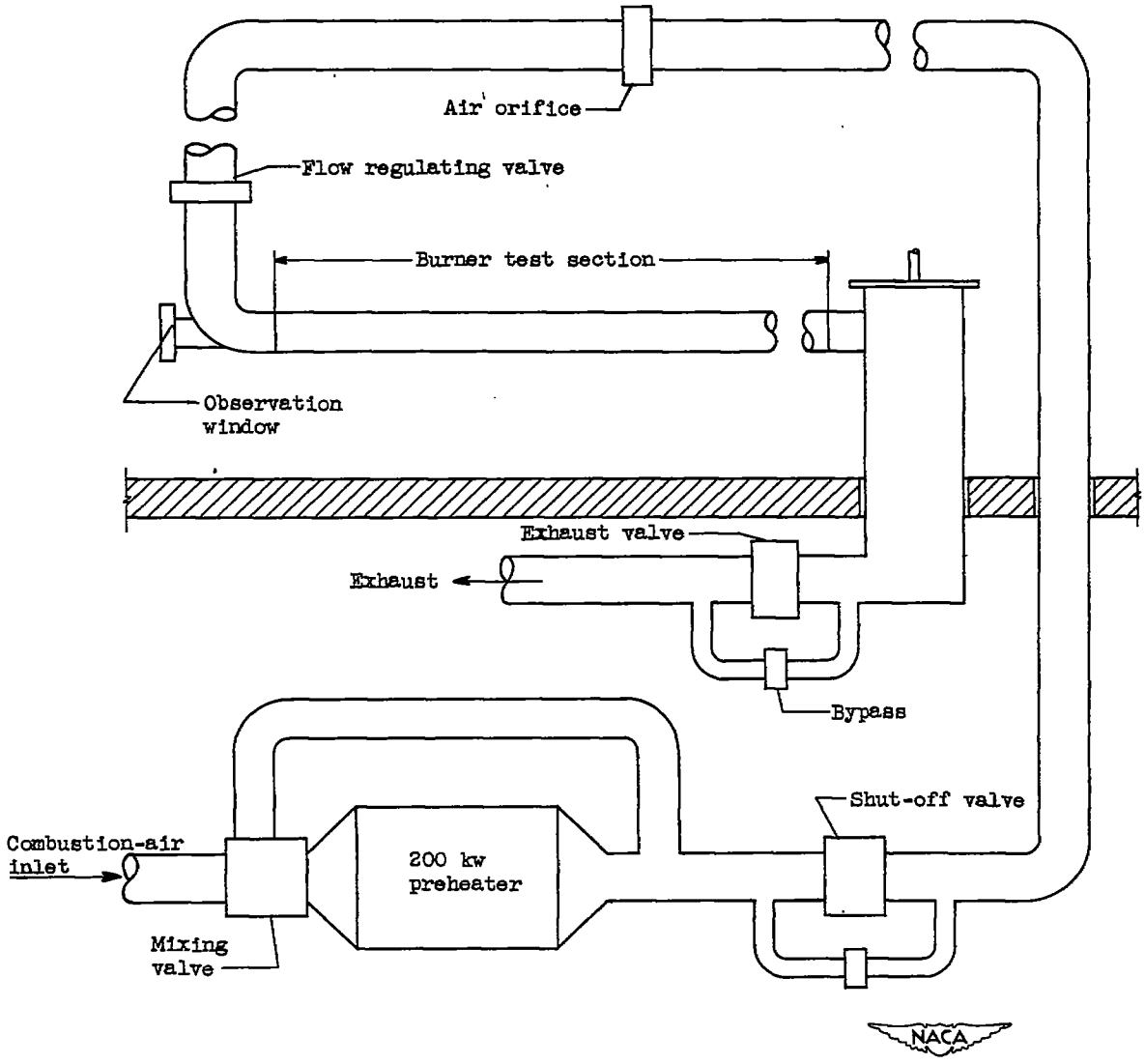

Figure 1. - General combustion-air system.

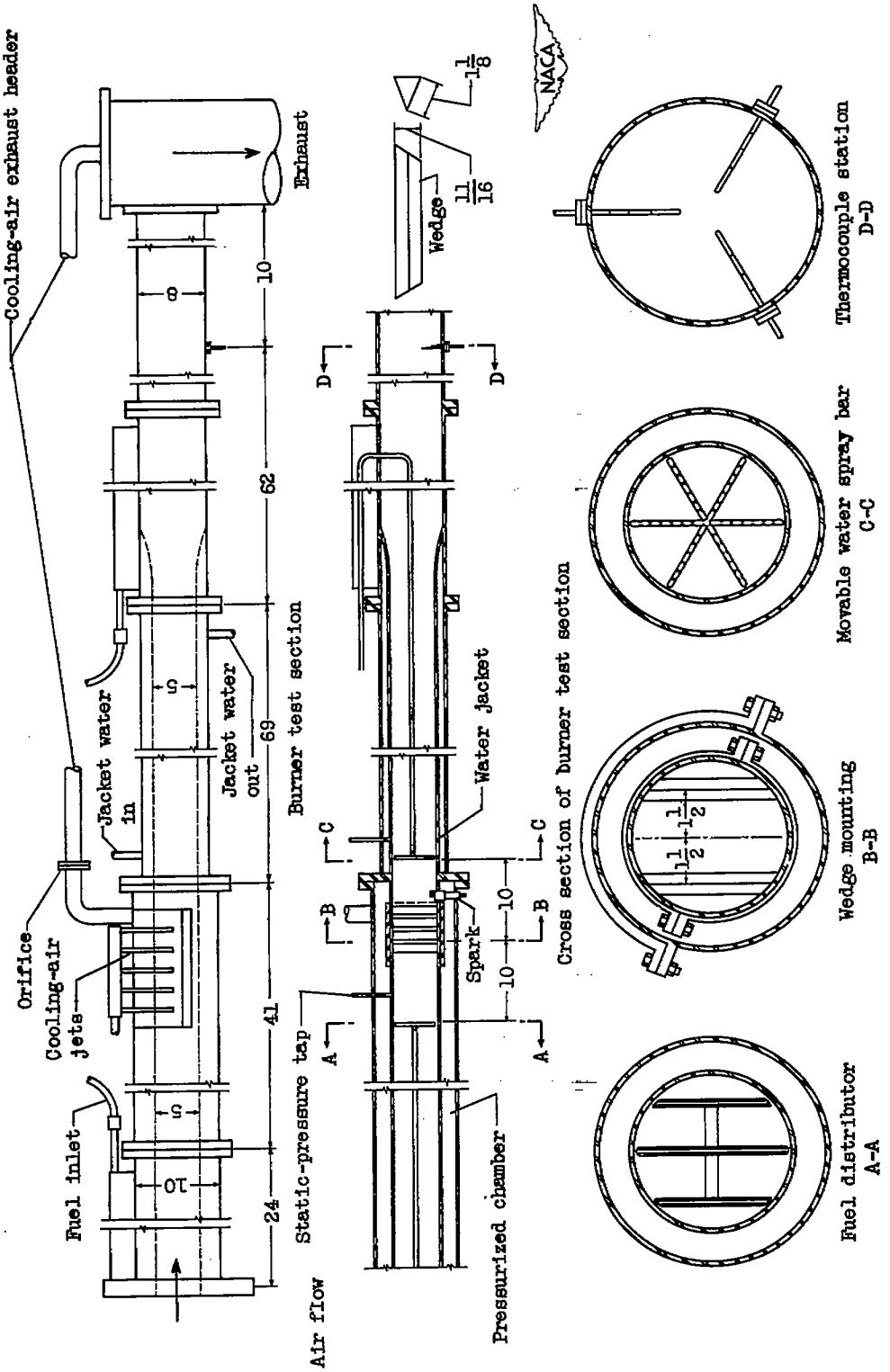

Figure 2. - Immersed wedge burner layout. (All dimensions in inches.)

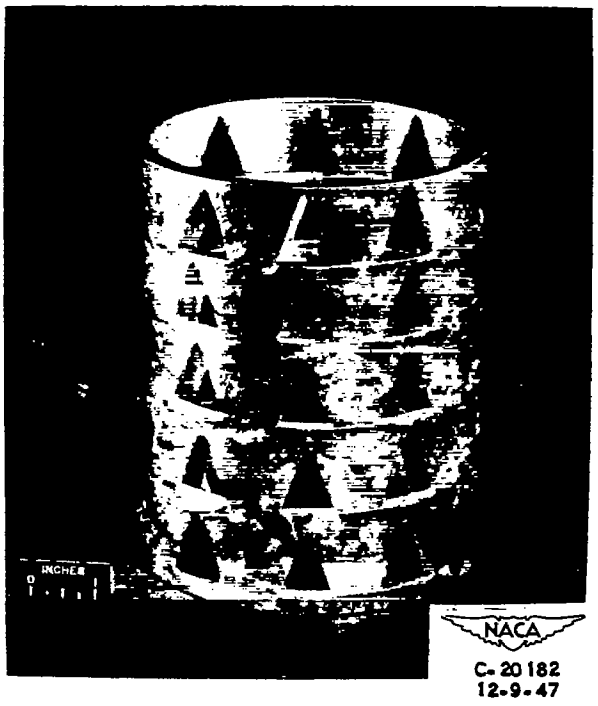

(a) Side view.

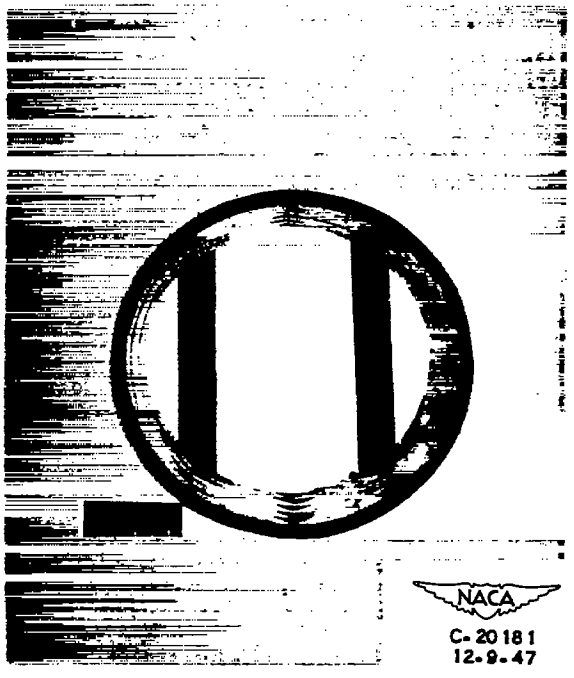

(b) Axial view.

Figure 3. - Wedge holder with one row in place.

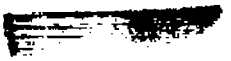

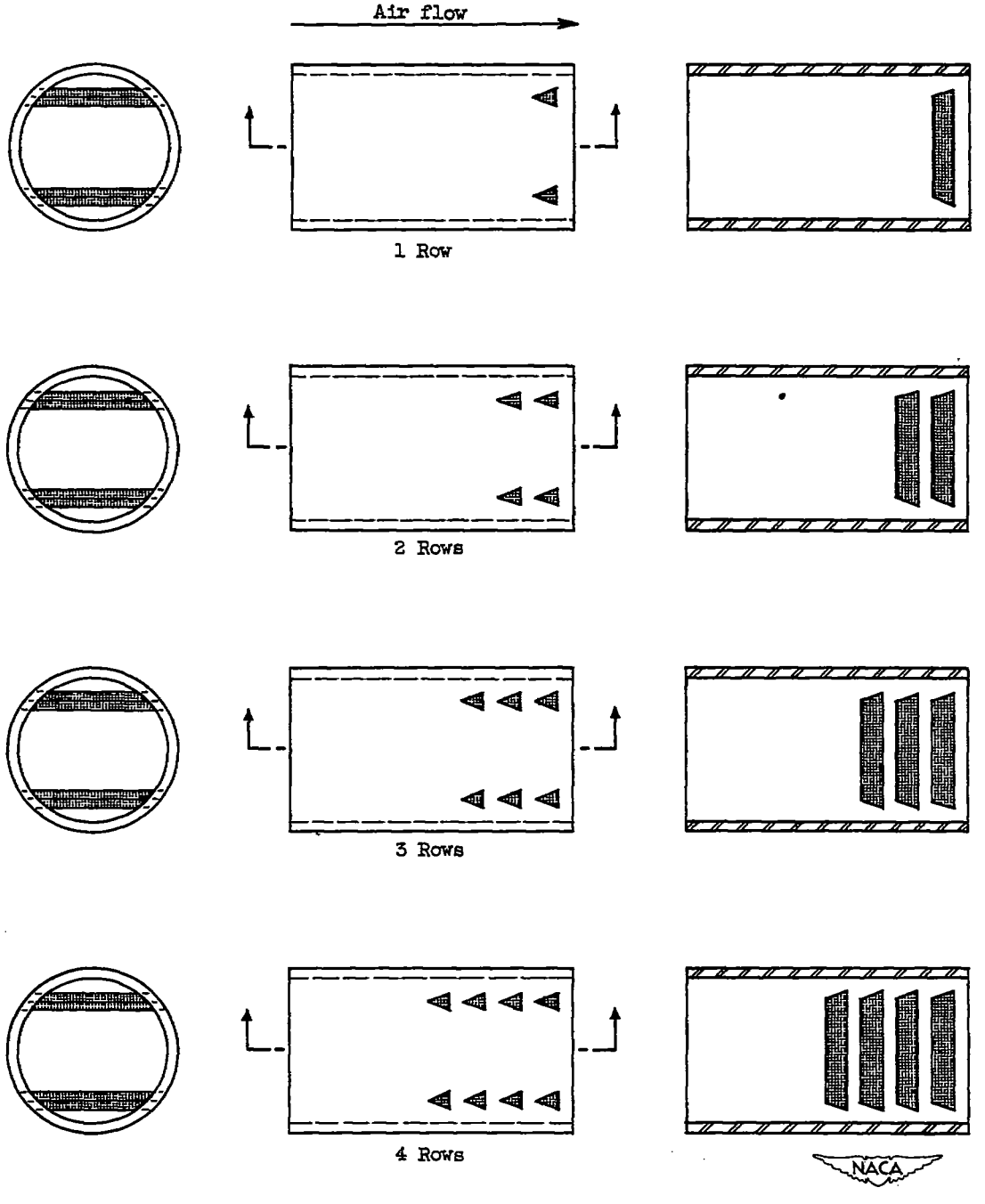

Figure 4. - Wedge positions for various combustion-chamber configurations.

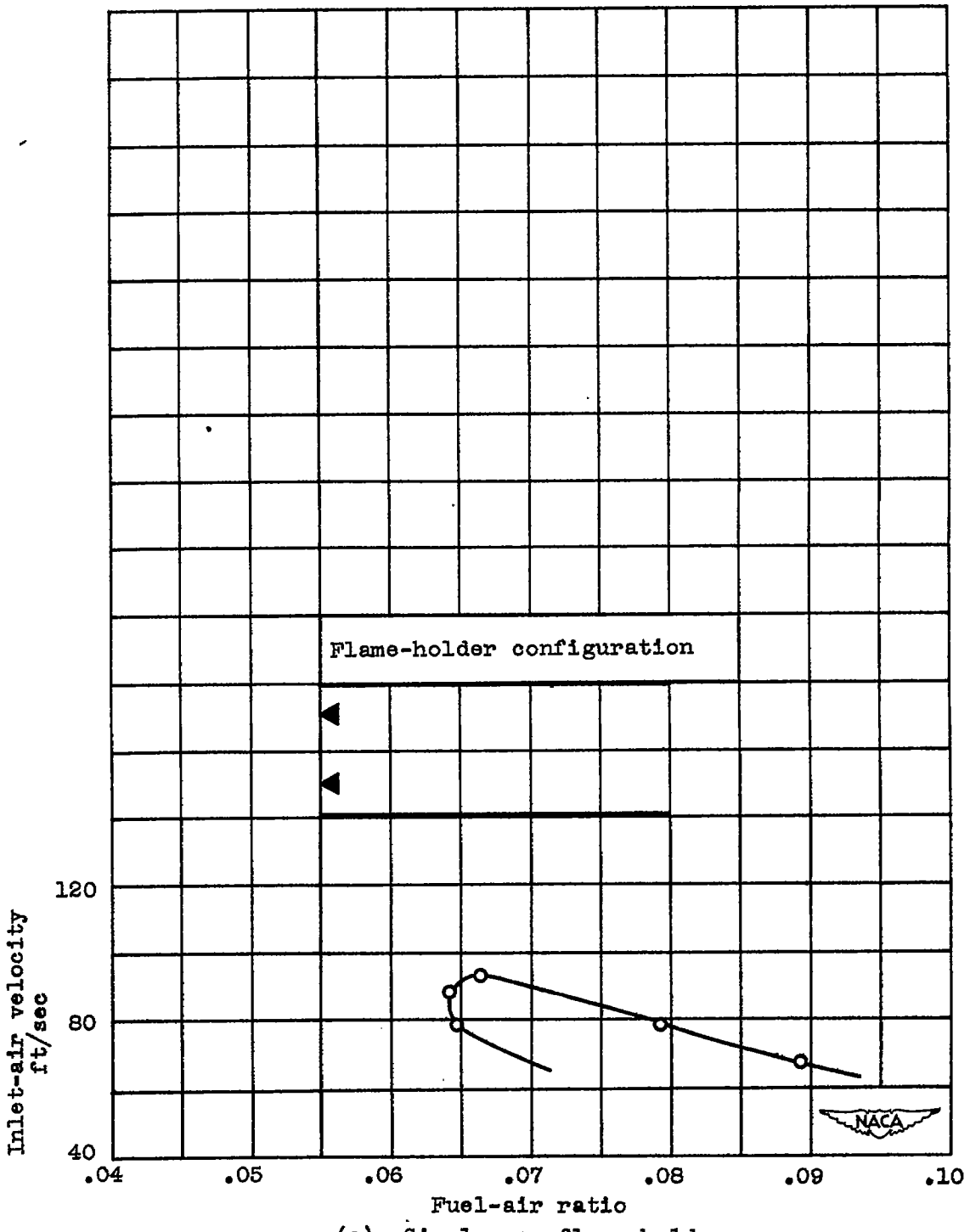

(a) Single-row flame holder.

Figure 6. - Ram-jet combustion-chamber altitude stability limits. Inlet-air pressure, 40 inches mercury absolute; inlet-air temperature, 120° F.

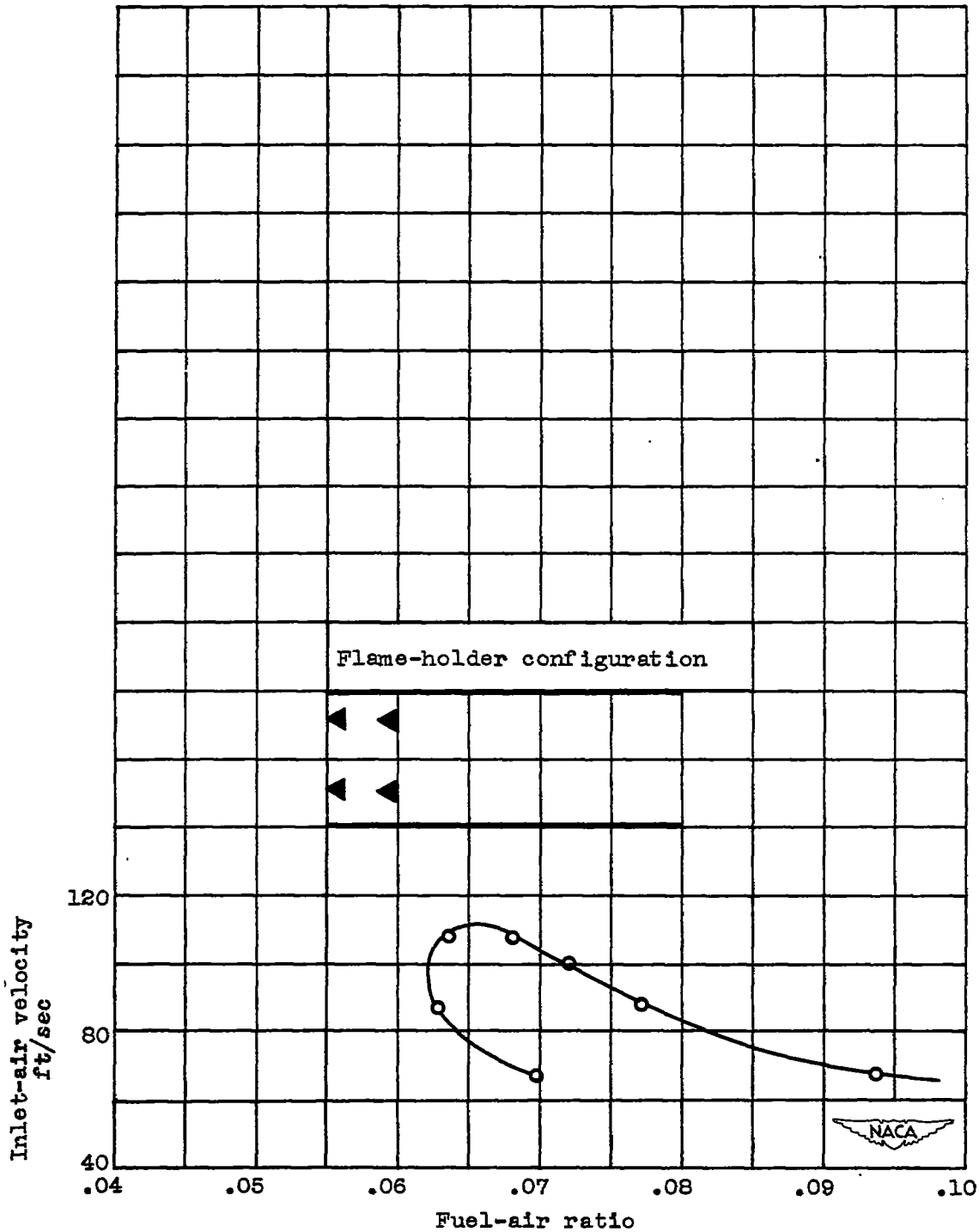

(b) Two-row flame holder.

Figure 5. - Continued. Ram-jet combustion-chamber altitude stability limits. Inlet-air pressure, 40 inches mercury absolute; inlet-air temperature, 120° F.

[redacted]

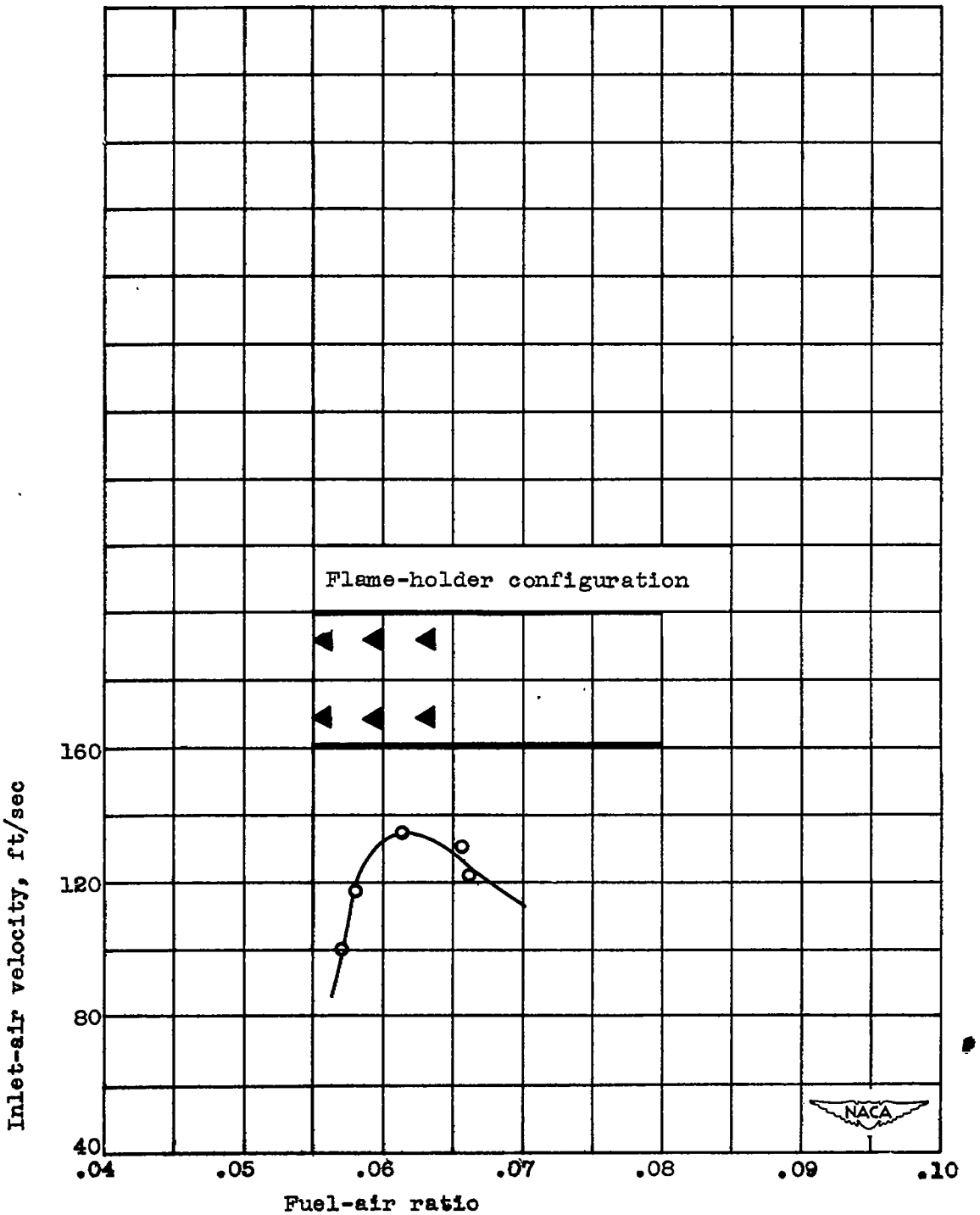

(c) Three-row flame holder.

Figure 5. - Continued. Ram-jet combustion-chamber altitude stability limits. Inlet-air pressure, 40 inches mercury absolute; inlet-air temperature, 120° F.

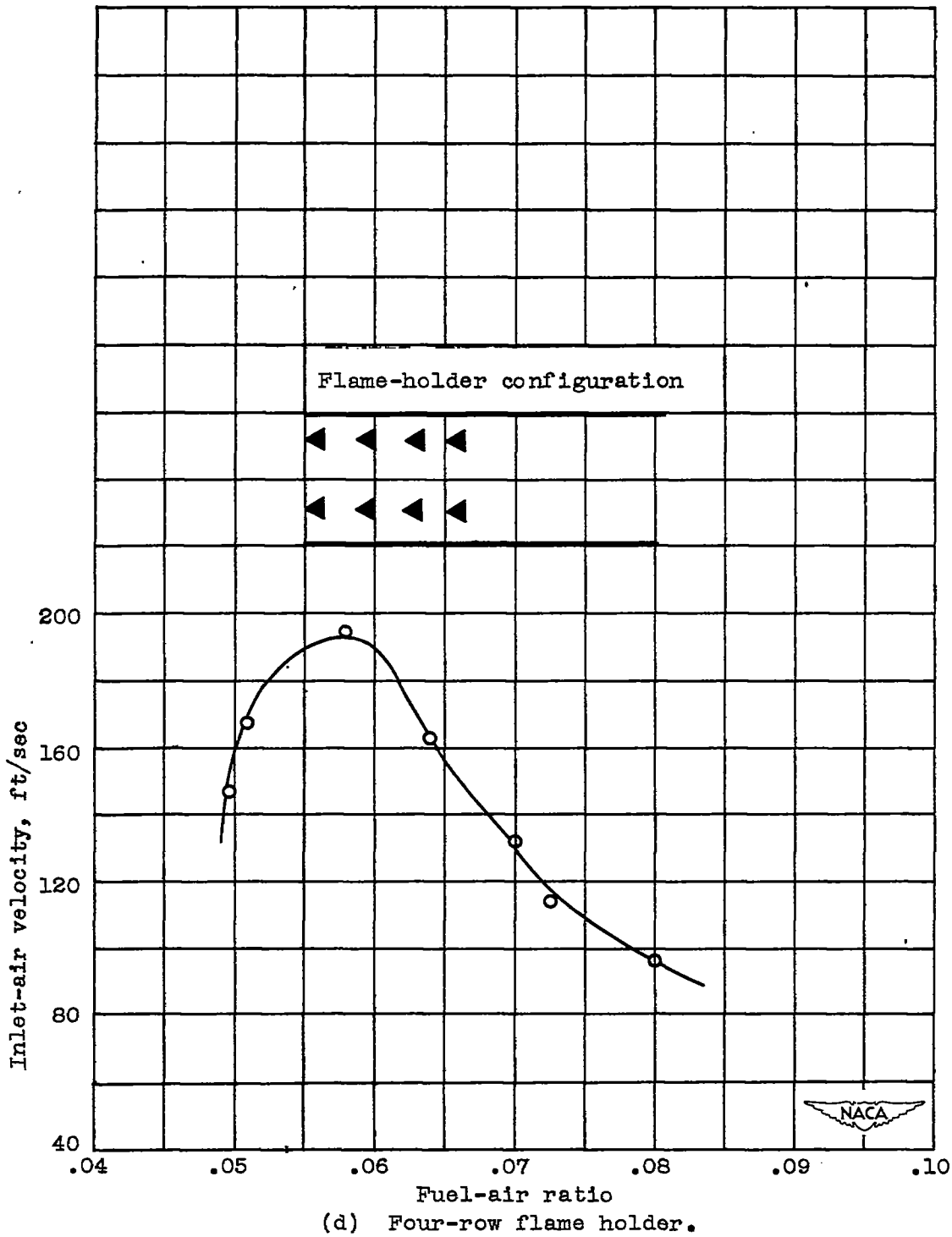

(d) Four-row flame holder.

Figure 5. - Continued. Ram-jet combustion-chamber altitude stability limits. Inlet-air pressure, 40 inches mercury absolute; inlet-air temperature, 120° F.

[redacted]

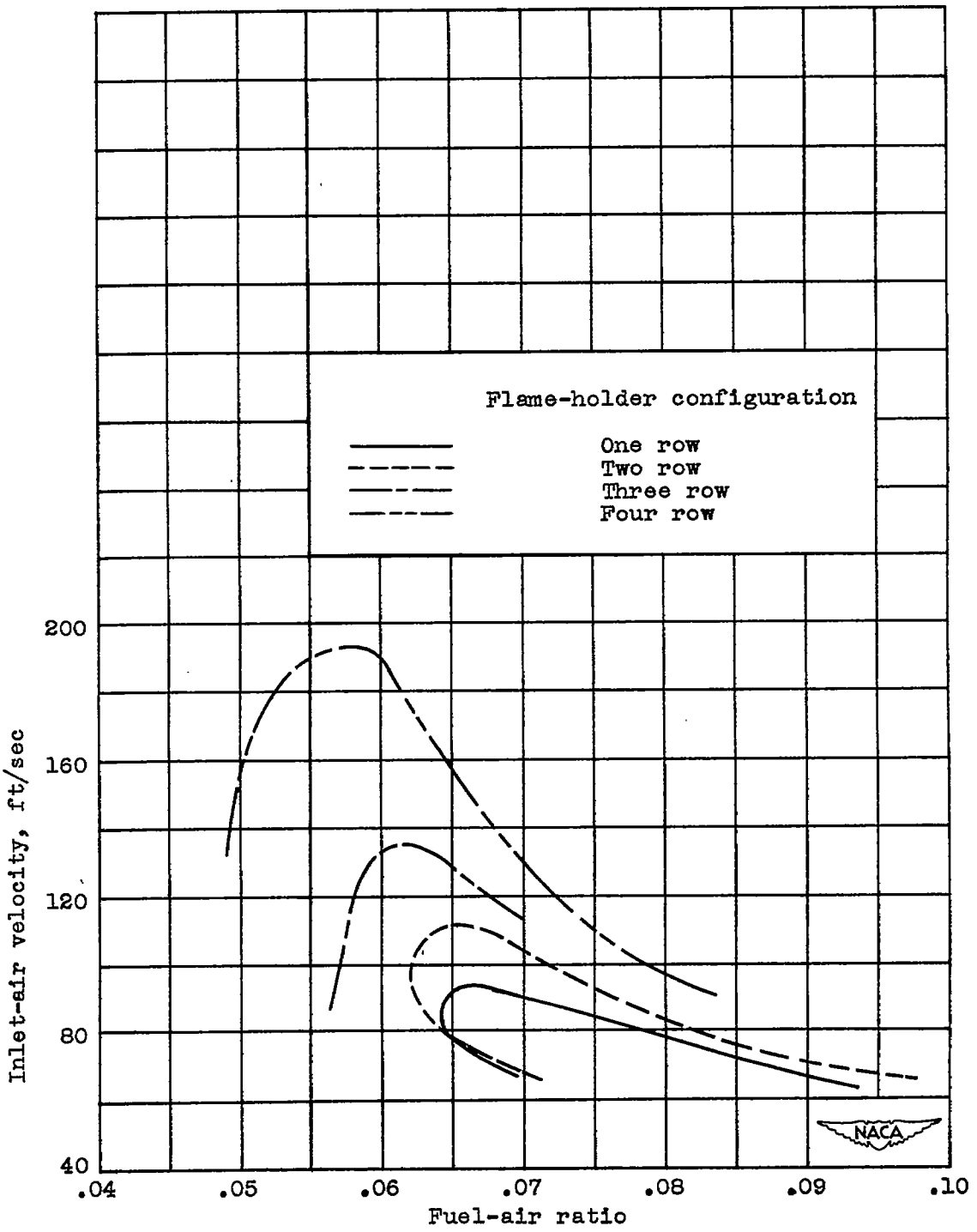

(e) One-, two-, three-, and four-row flame holders.

Figure 5. - Continued. Ram-jet combustion-chamber altitude stability limits. Inlet-air pressure, 40 inches mercury absolute; inlet-air temperature, 120° F.

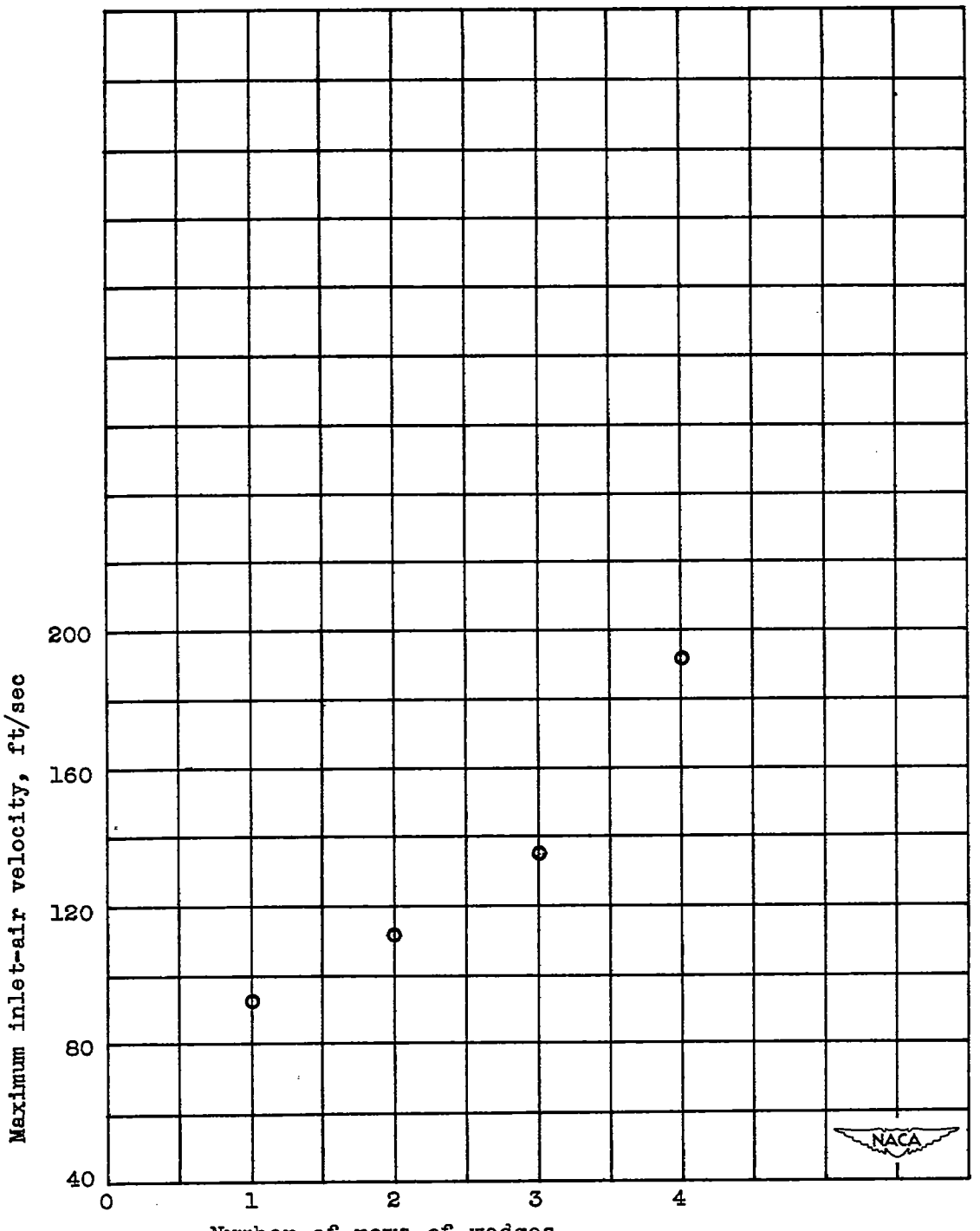

(f) Maximum allowable inlet-air velocity.

Figure 5. - Concluded. Ram-jet combustion-chamber altitude stability limits. Inlet-air pressure, 40 inches mercury absolute; inlet-air temperature, 120° F.

[redacted]

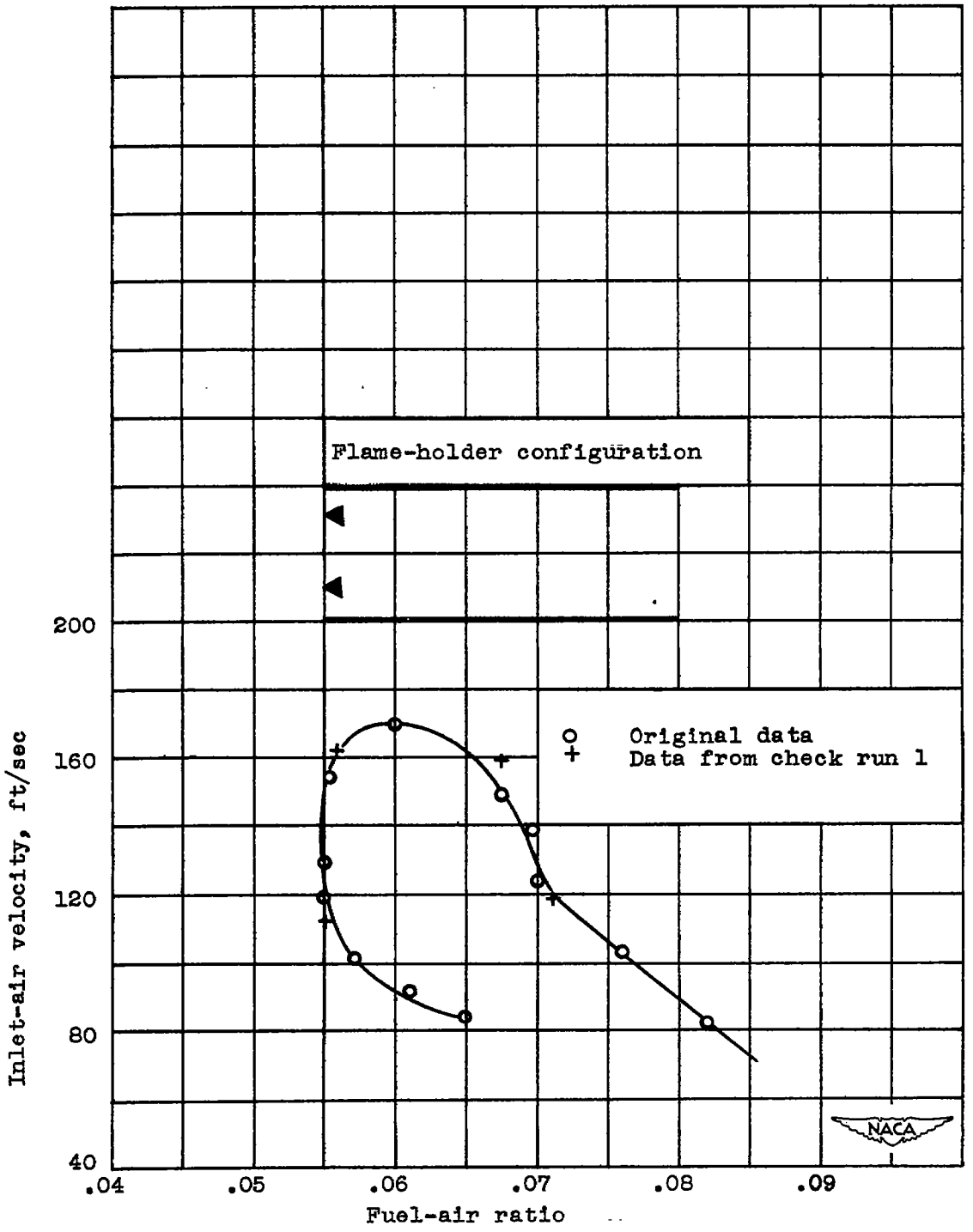

(a) Single-row flame holder.

Figure 6. - Ram-jet combustion-chamber sea-level stability limits. Inlet-air pressure, 55 inches mercury absolute; inlet-air temperature, 160° F.

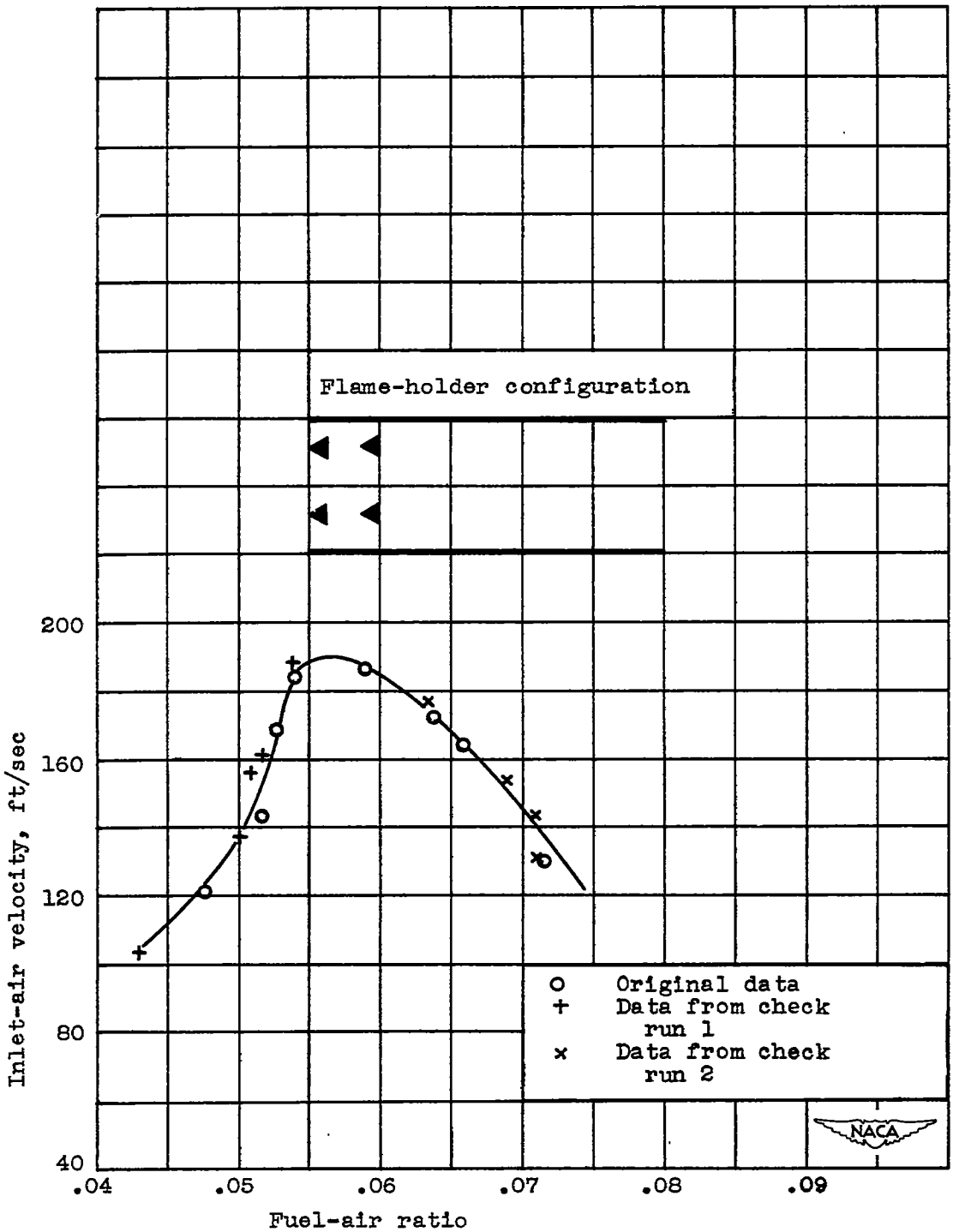

(b) Two-row flame holder.

Figure 6. - Continued. Ram-jet combustion-chamber sea-level stability limits. Inlet-air pressure, 55 inches mercury absolute; inlet-air temperature, 160° F.

[redacted]

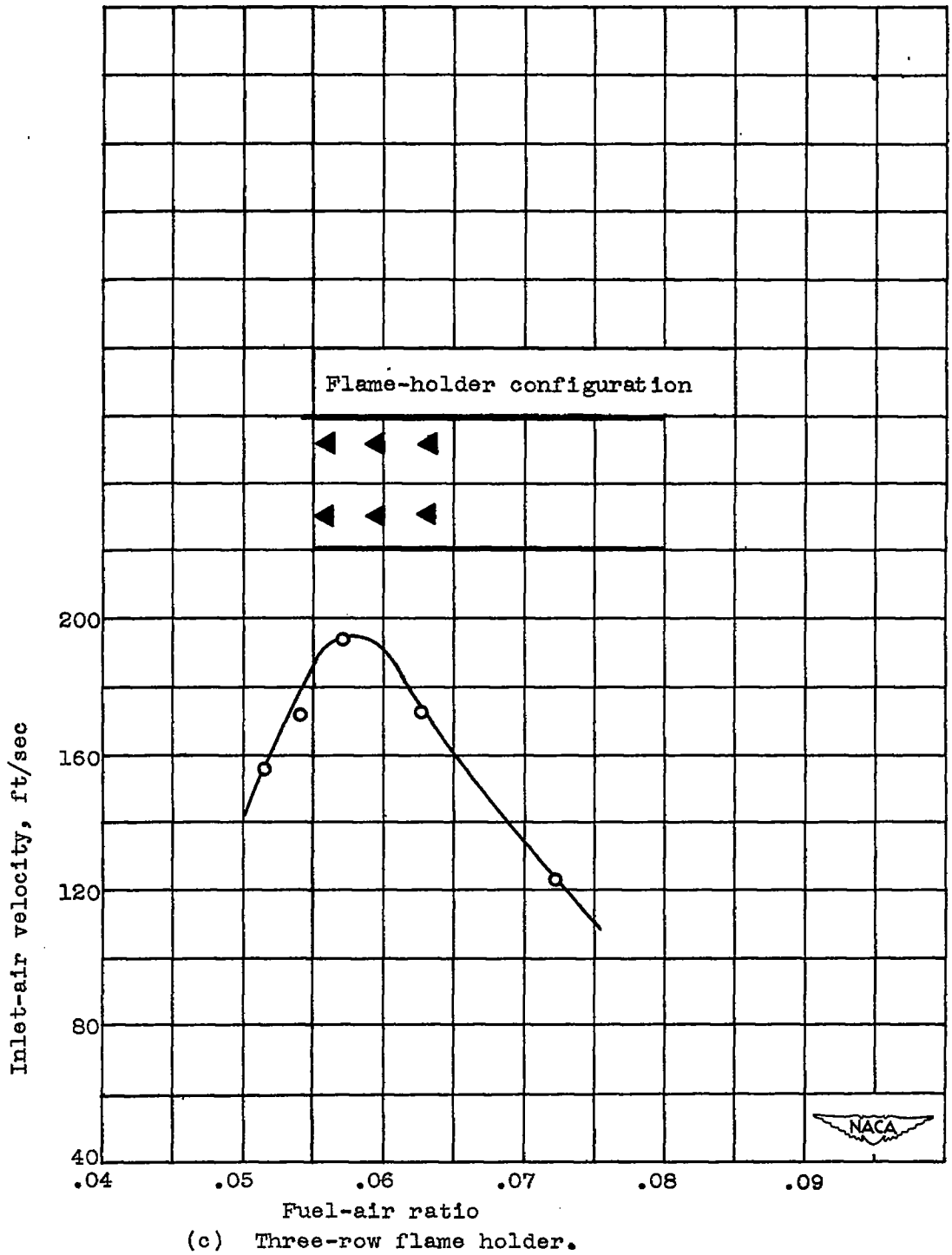

(c) Three-row flame holder.

Figure 6. - Continued. Ram-jet combustion-chamber sea-level stability limits. Inlet-air pressure, 55 inches mercury absolute; inlet-air temperature, 160° F.

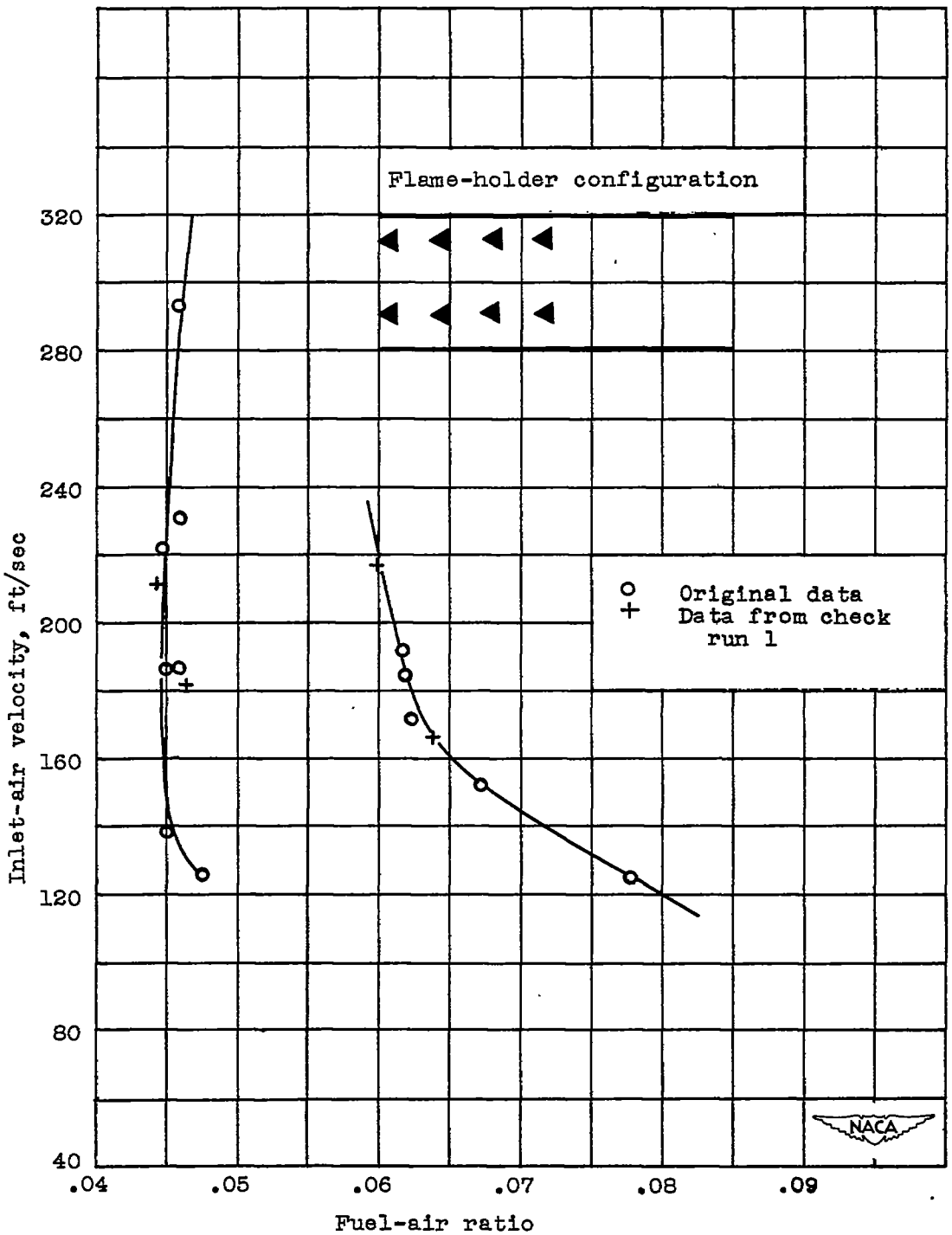

(d) Four-row flame holder.

Figure 6. - Continued. Ram-jet combustion-chamber sea-level stability limits. Inlet-air pressure, 55 inches mercury absolute; inlet-air temperature, 160° F.

[redacted]

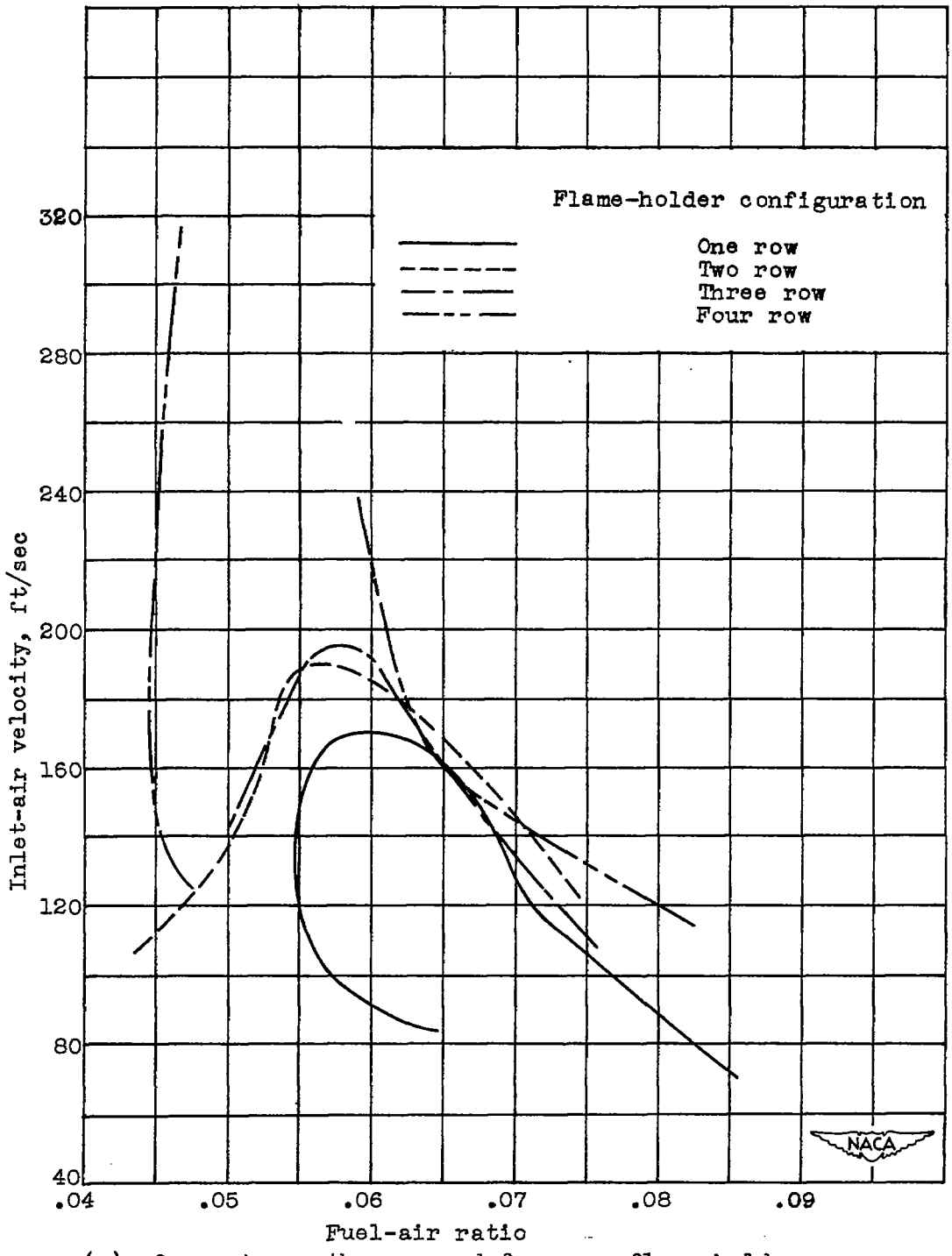

(e) One-, two-, three-, and four-row flame holders.

Figure 6. - Continued. Ram-jet combustion-chamber sea-level stability limits. Inlet-air pressure, 55 inches mercury absolute; inlet-air temperature, 160° F.

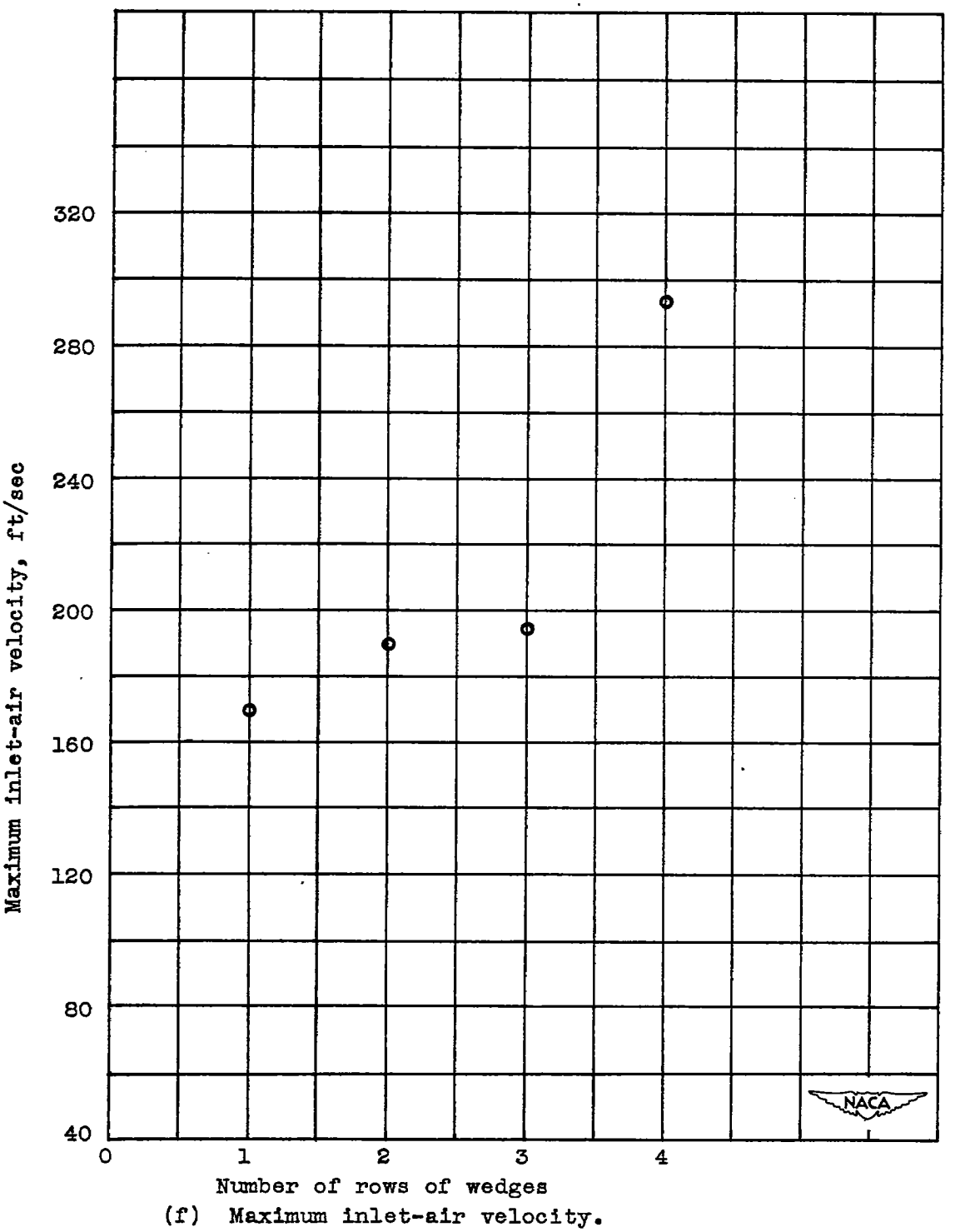

(f) Maximum inlet-air velocity.

Figure 6. - Concluded. Ram-jet combustion-chamber sea-level stability limits. Inlet-air pressure, 55 inches mercury absolute; inlet-air temperature, 160° F.

[redacted]

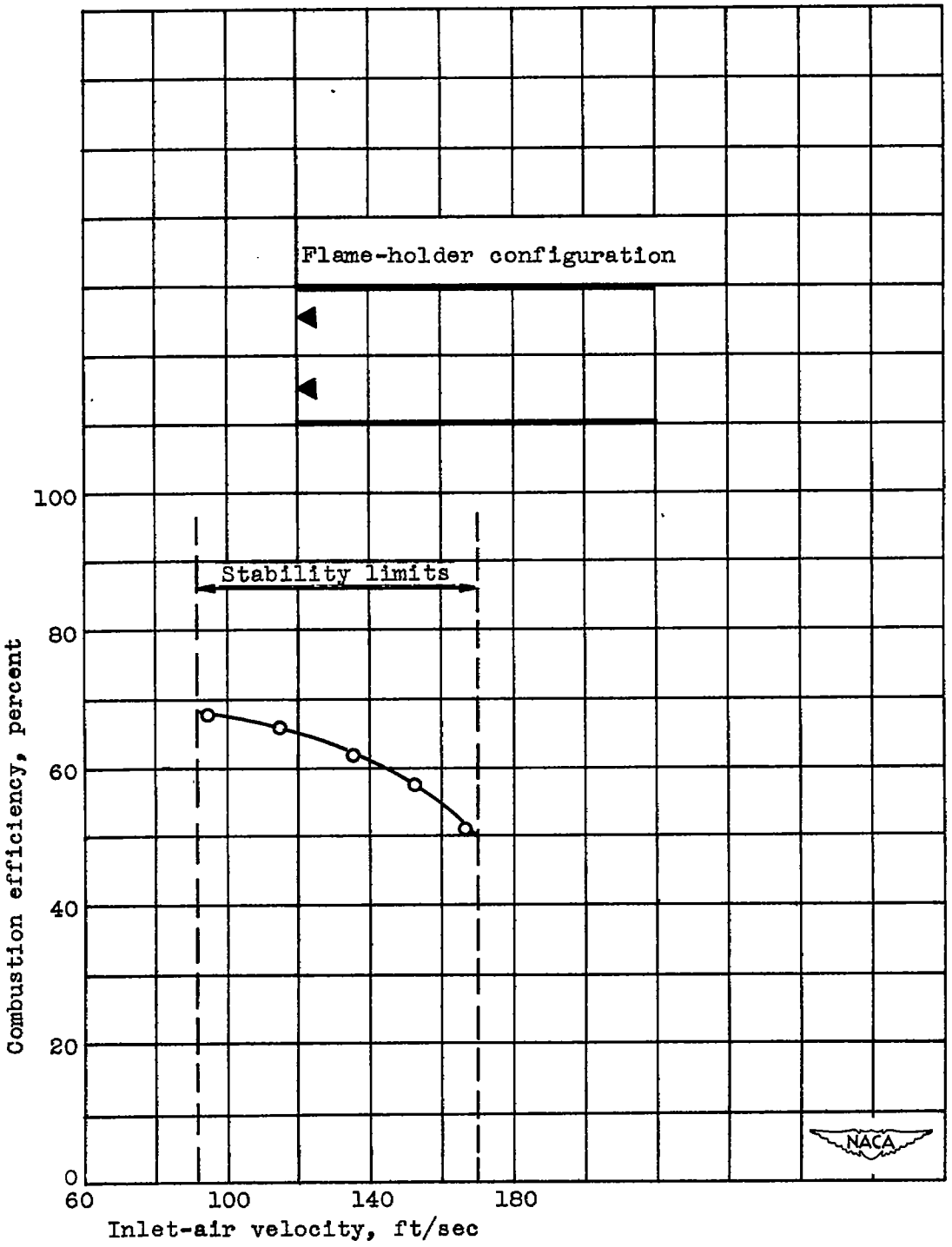

Figure 7. - Effect of inlet-air velocity on combustion efficiency of single-row configuration at simulated sea-level conditions. Inlet-air pressure, 55 inches mercury absolute; inlet-air temperature, 160° F; fuel-air ratio, 0.06.

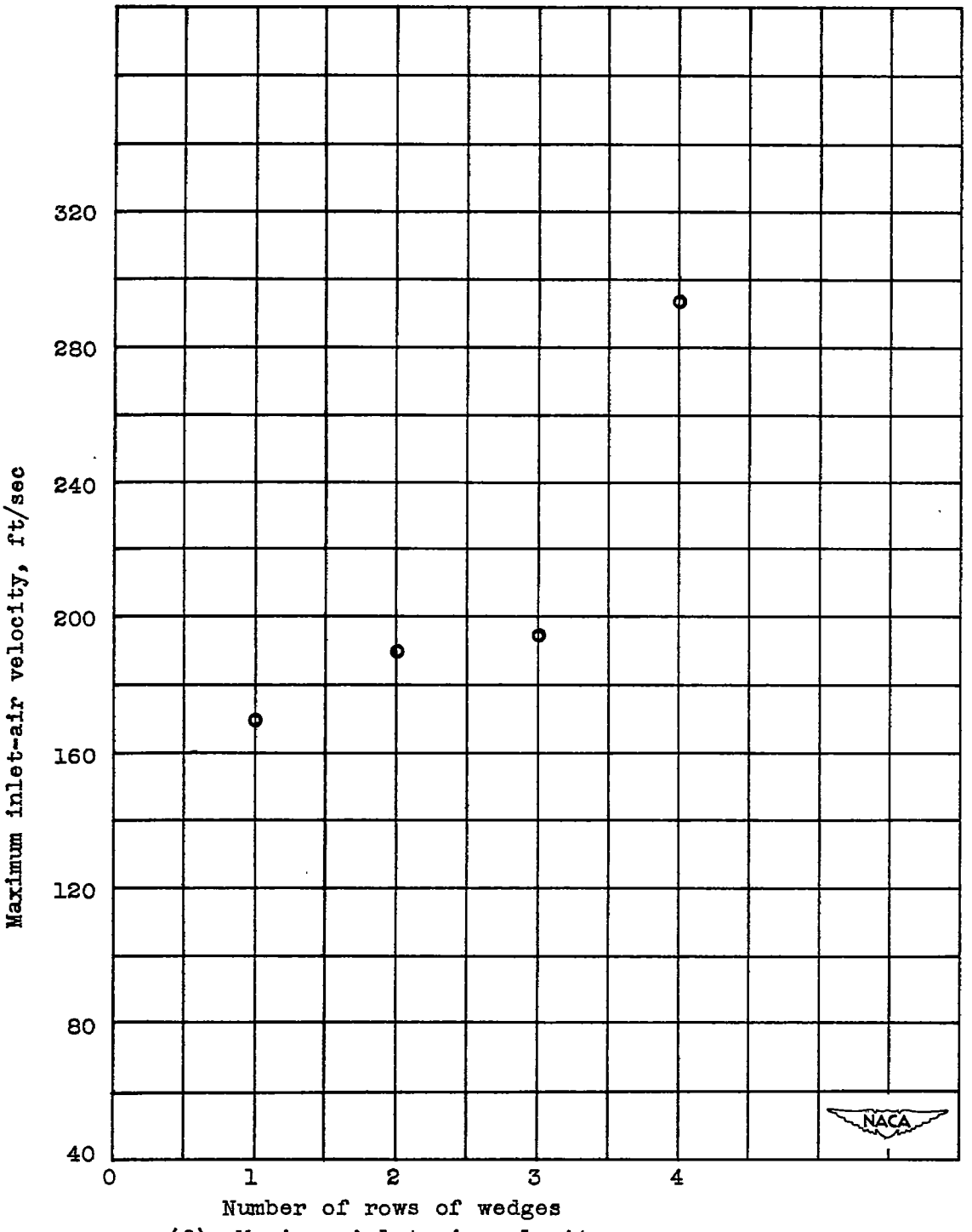

(f) Maximum inlet-air velocity.

Figure 6. - Concluded. Ram-jet combustion-chamber sea-level stability limits. Inlet-air pressure, 55 inches mercury absolute; inlet-air temperature, 160° F.

[redacted]

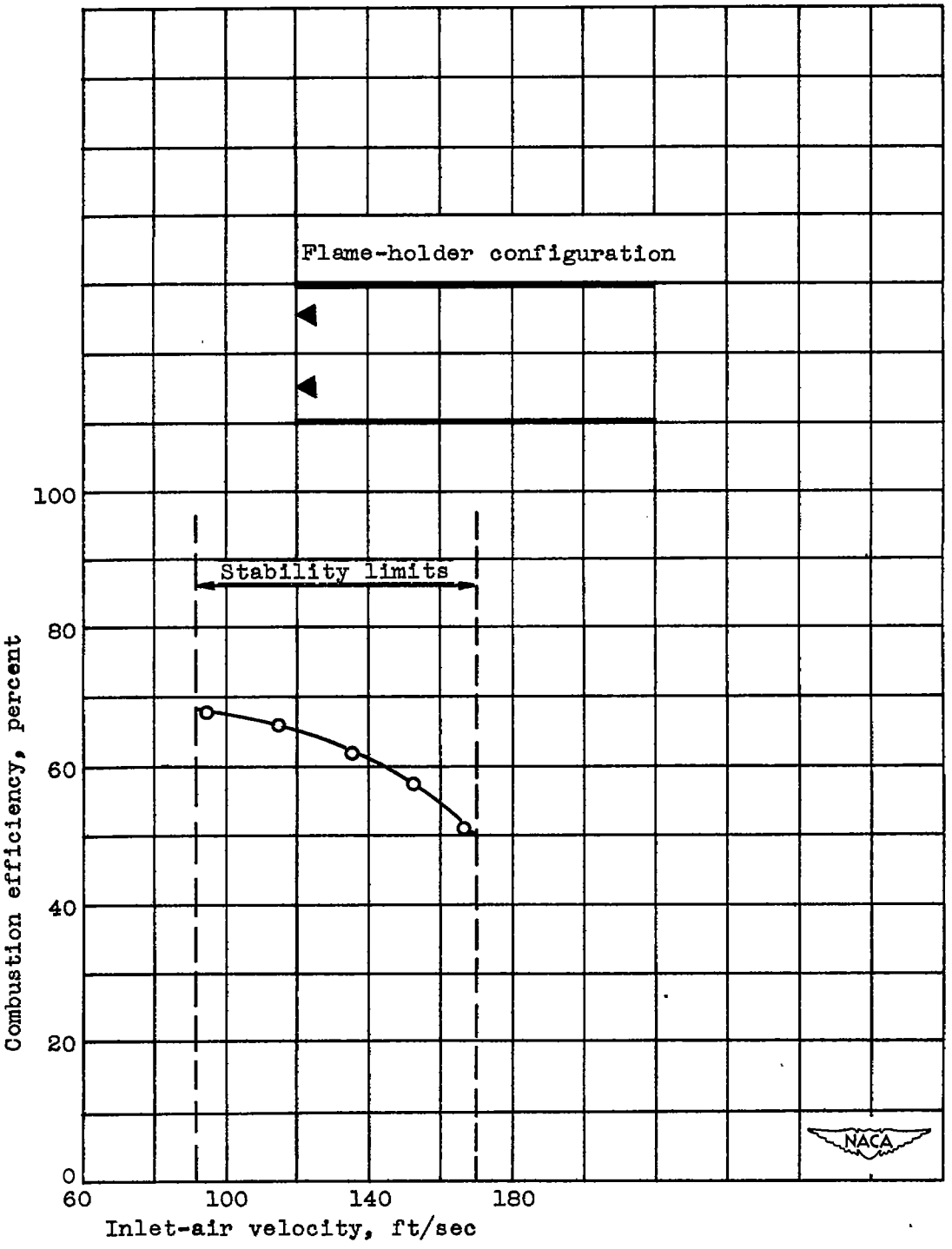

Figure 7. - Effect of inlet-air velocity on combustion efficiency of single-row configuration at simulated sea-level conditions. Inlet-air pressure, 55 inches mercury absolute; inlet-air temperature, 160° F; fuel-air ratio, 0.06.

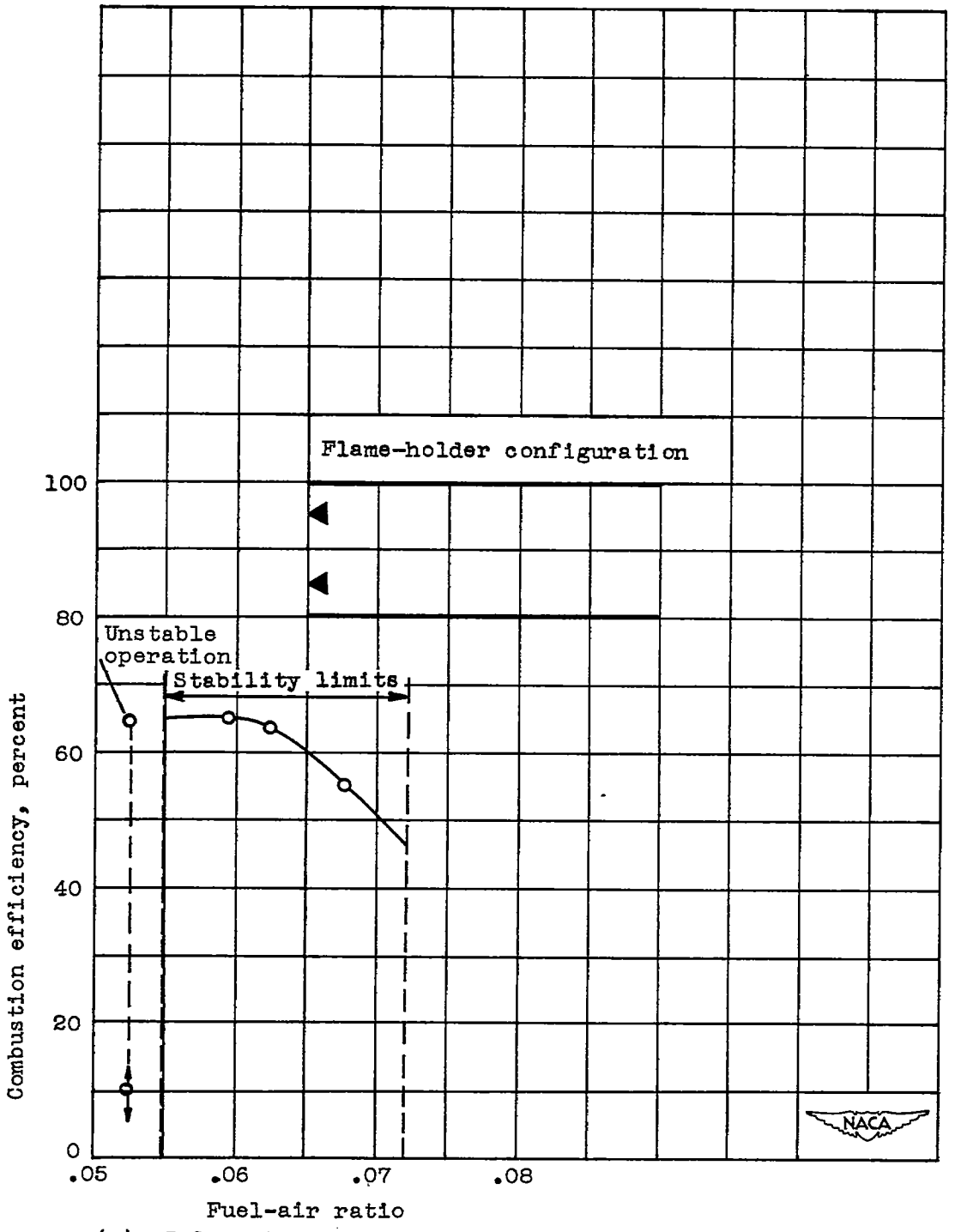

(a) Inlet-air velocity, 115 feet per second.

Figure 8. - Effect of fuel-air ratio on combustion efficiency of single-row configuration at simulated sea-level conditions. Inlet-air pressure, 55 inches mercury absolute; inlet-air temperature, 160° F.

[redacted]

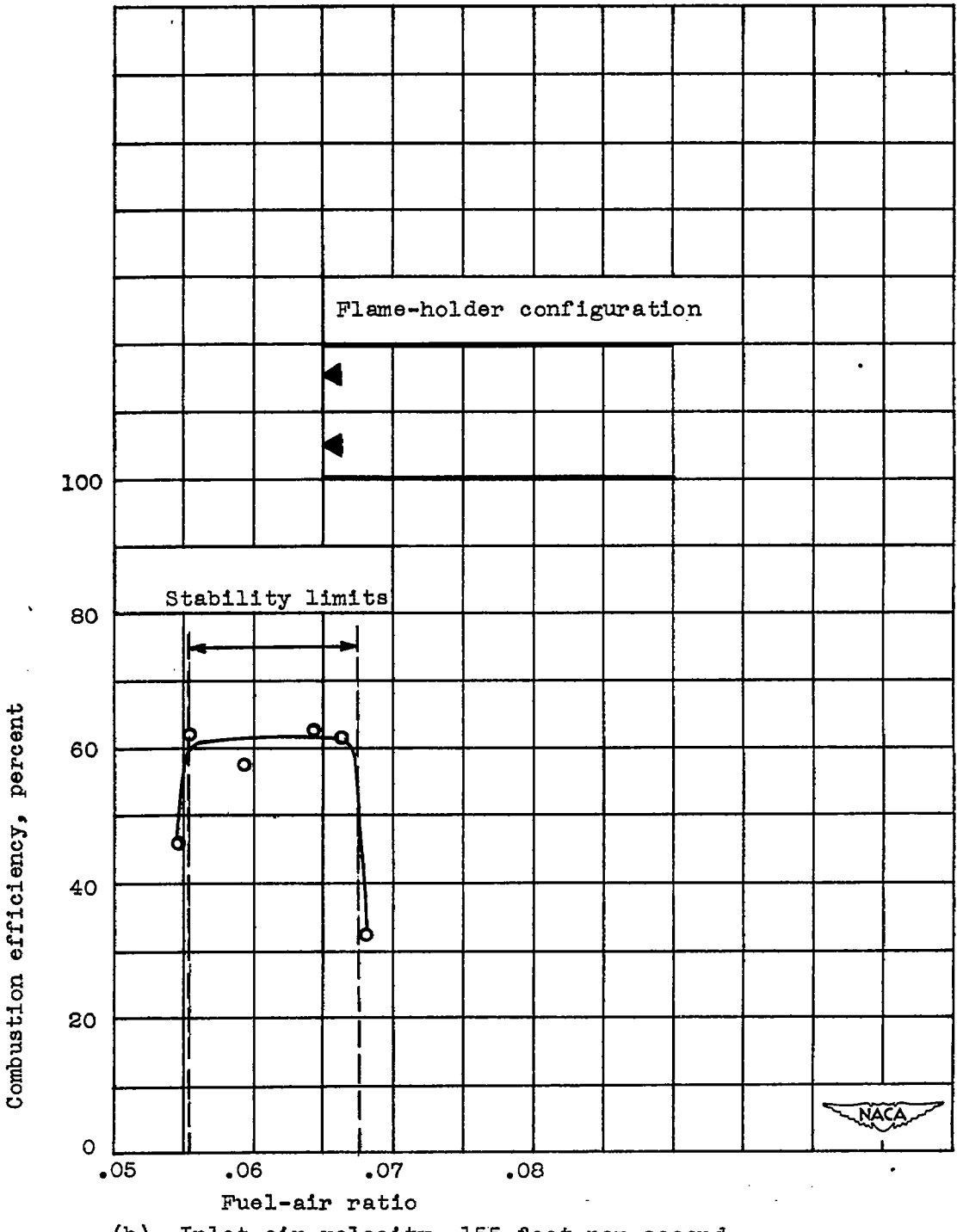

(b) Inlet-air velocity, 155 feet per second.

Figure 8. - Concluded. Effect of fuel-air ratio on combustion efficiency of single-row configuration at simulated sea-level conditions. Inlet-air pressure, 55 inches mercury absolute; inlet-air temperature, 160° F.

[redacted]

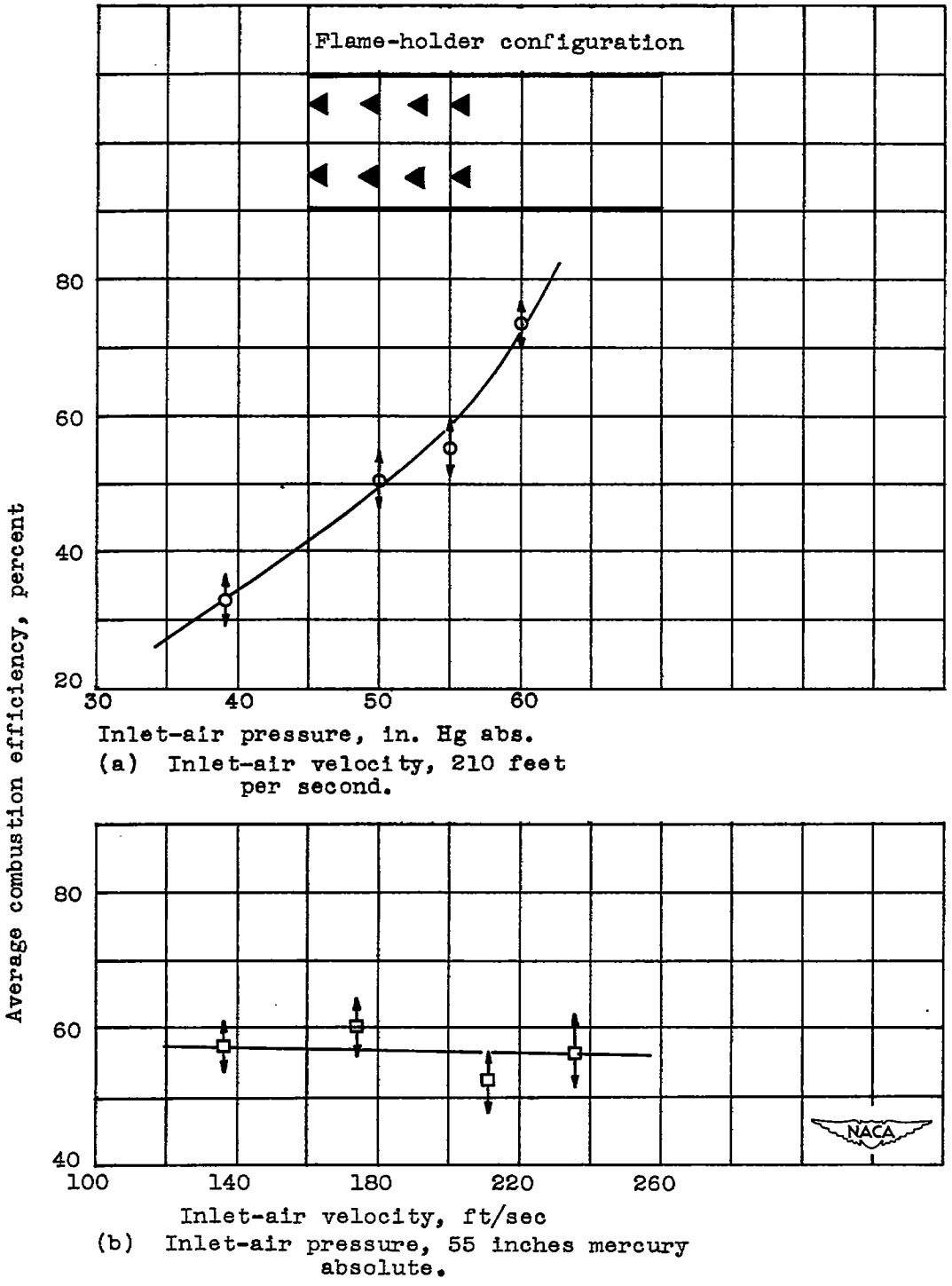

Figure 9. - Effect of inlet-air velocity and inlet-air pressure on combustion efficiency of four-row configuration at simulated sea-level conditions. Inlet-air temperature, 160° F; fuel-air ratio, 0.0505 to 0.0550.

[redacted]

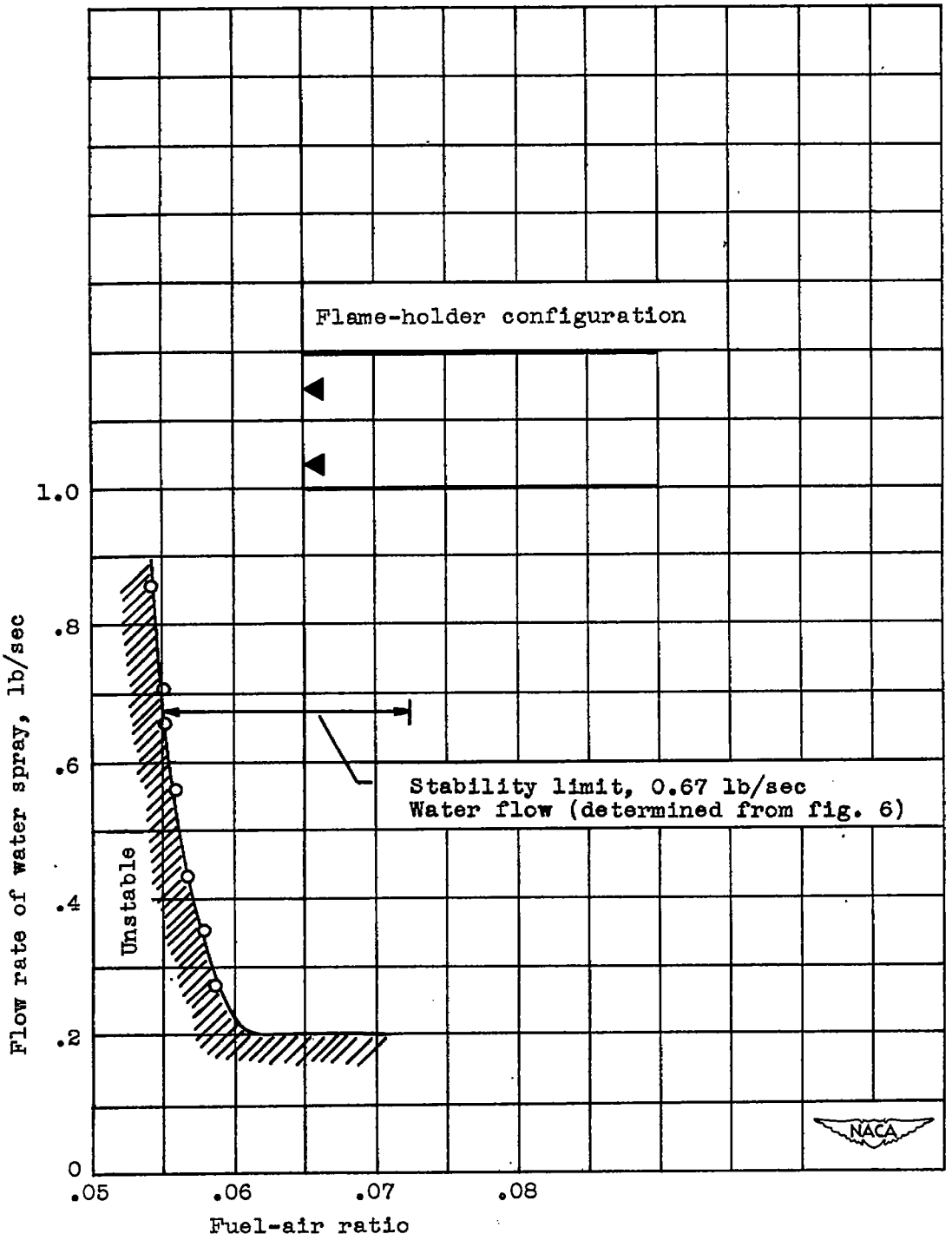

Figure 10. - Effect of rate of water flow to quenching spray on stability limit at simulated sea-level conditions. Inlet-air velocity, 115 feet per second; inlet-air pressure, 55 inches mercury absolute; inlet-air temperature, 160° F.

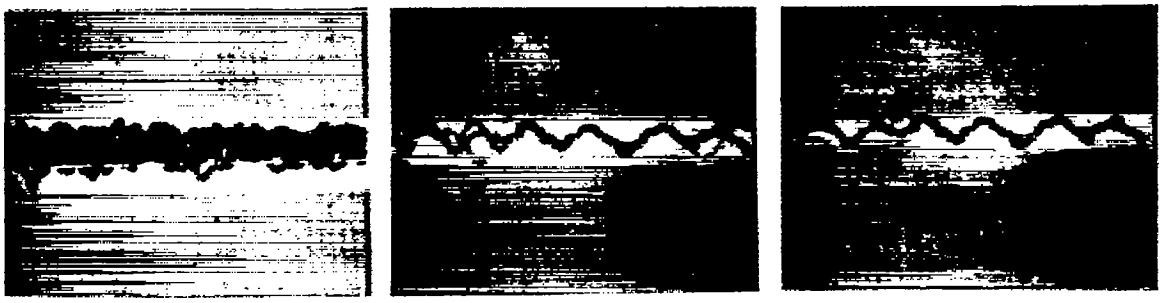

(a) Water flow rate, 0.80 pound per second.

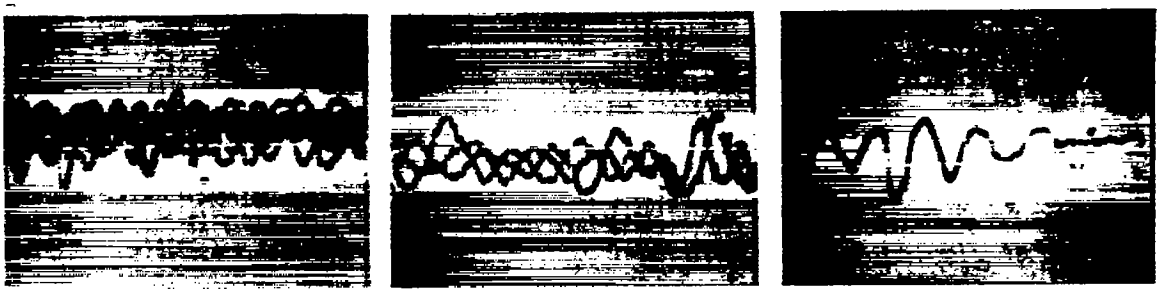

(b) Water flow rate, 0.60 pound per second.

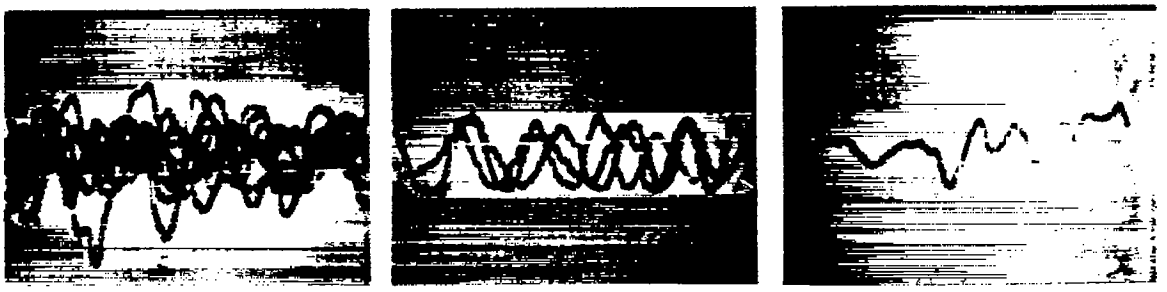

(c) Water flow rate, 0.40 pound per second.

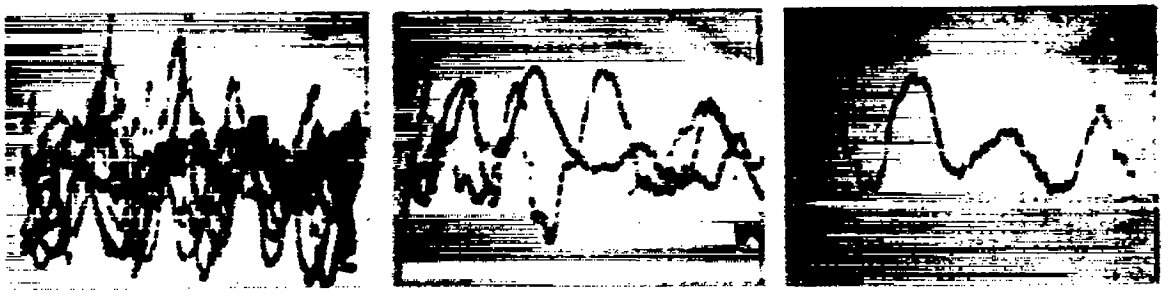

Exposure, 1 sec Exposure, 1/5 sec Exposure, 1/25 sec

(d) Water flow rate, 0.10 pound per second.

NACA C-21727 6-23-48

Figure 11. - Pressure-time oscillograph traces at various flow rates of water spray for single-row configuration. Inlet-air velocity, 120 feet per second; inlet-air pressure, 55 inches mercury absolute; inlet-air temperature, 160° F; fuel-air ratio, 0.06.

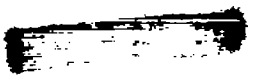

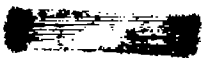

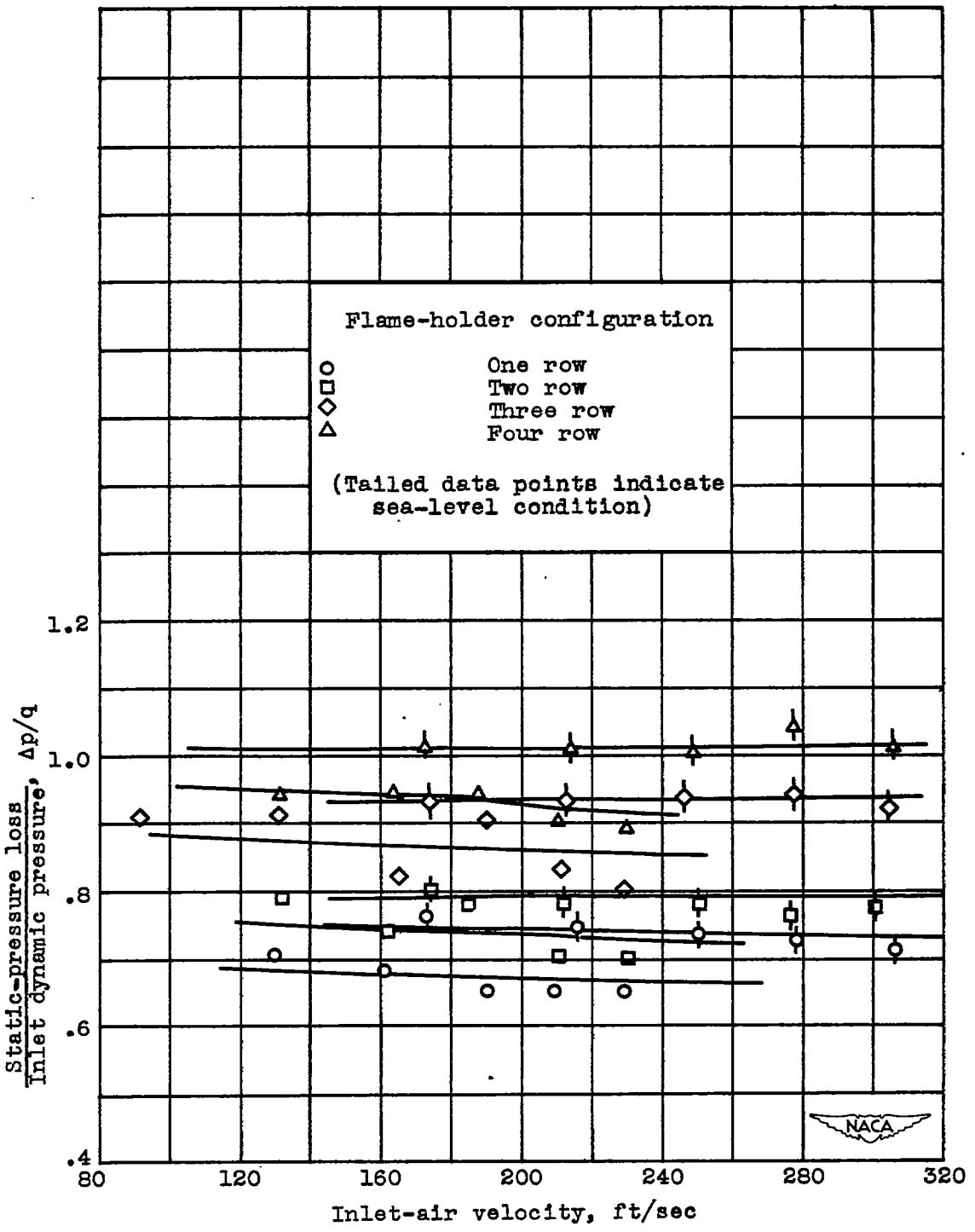

Figure 12. - Isothermal-pressure loss at simulated sea-level conditions of inlet-air pressure of 55 inches mercury absolute at inlet-air temperature of 160° F and altitude conditions of inlet-air pressure of 40 inches mercury absolute at inlet-air temperature of 120° F.

[redacted]

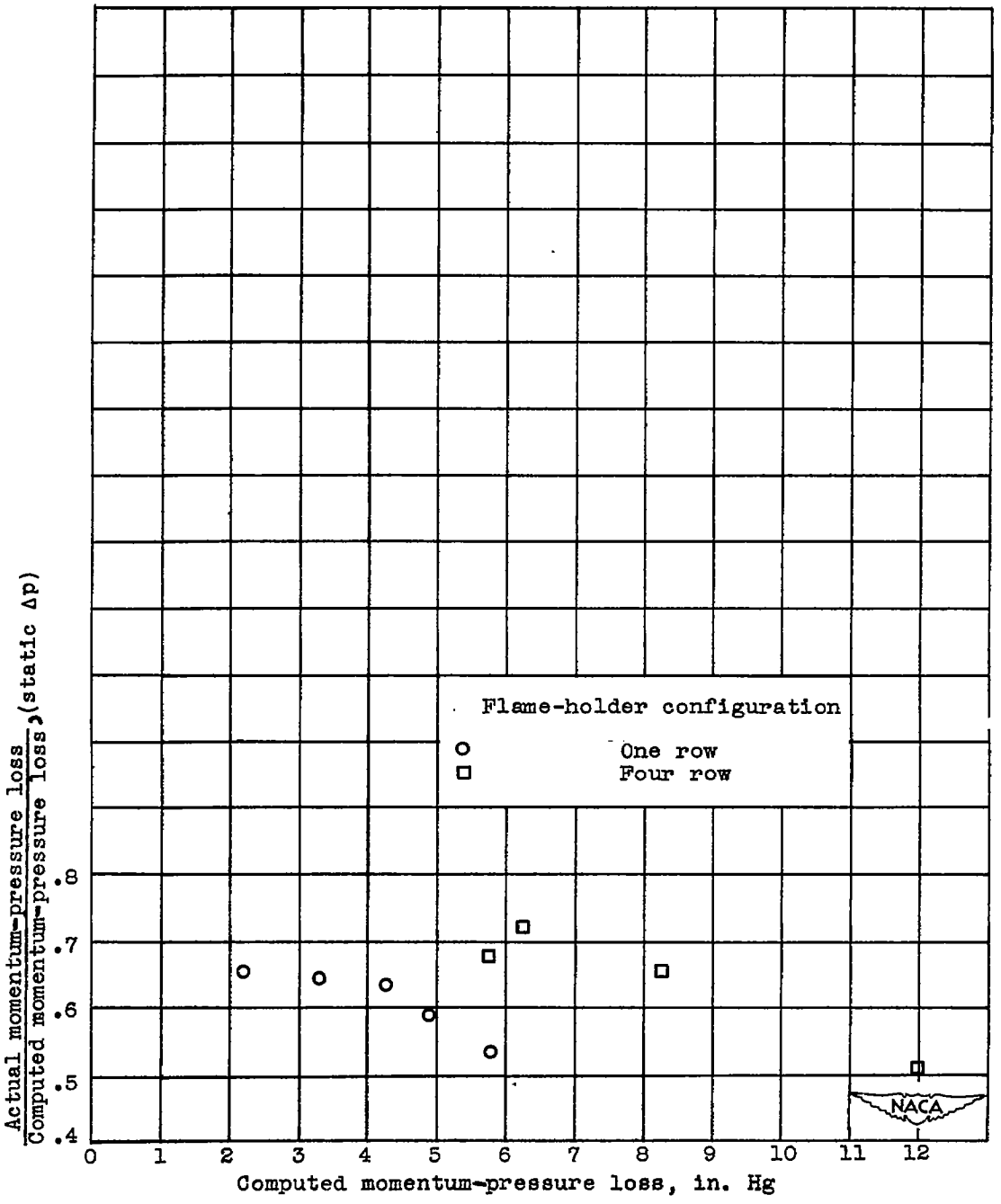

Figure 13. - Comparison of pressure losses for one- and four-row configurations at 55 inches mercury absolute and inlet-air temperature of 160° F.

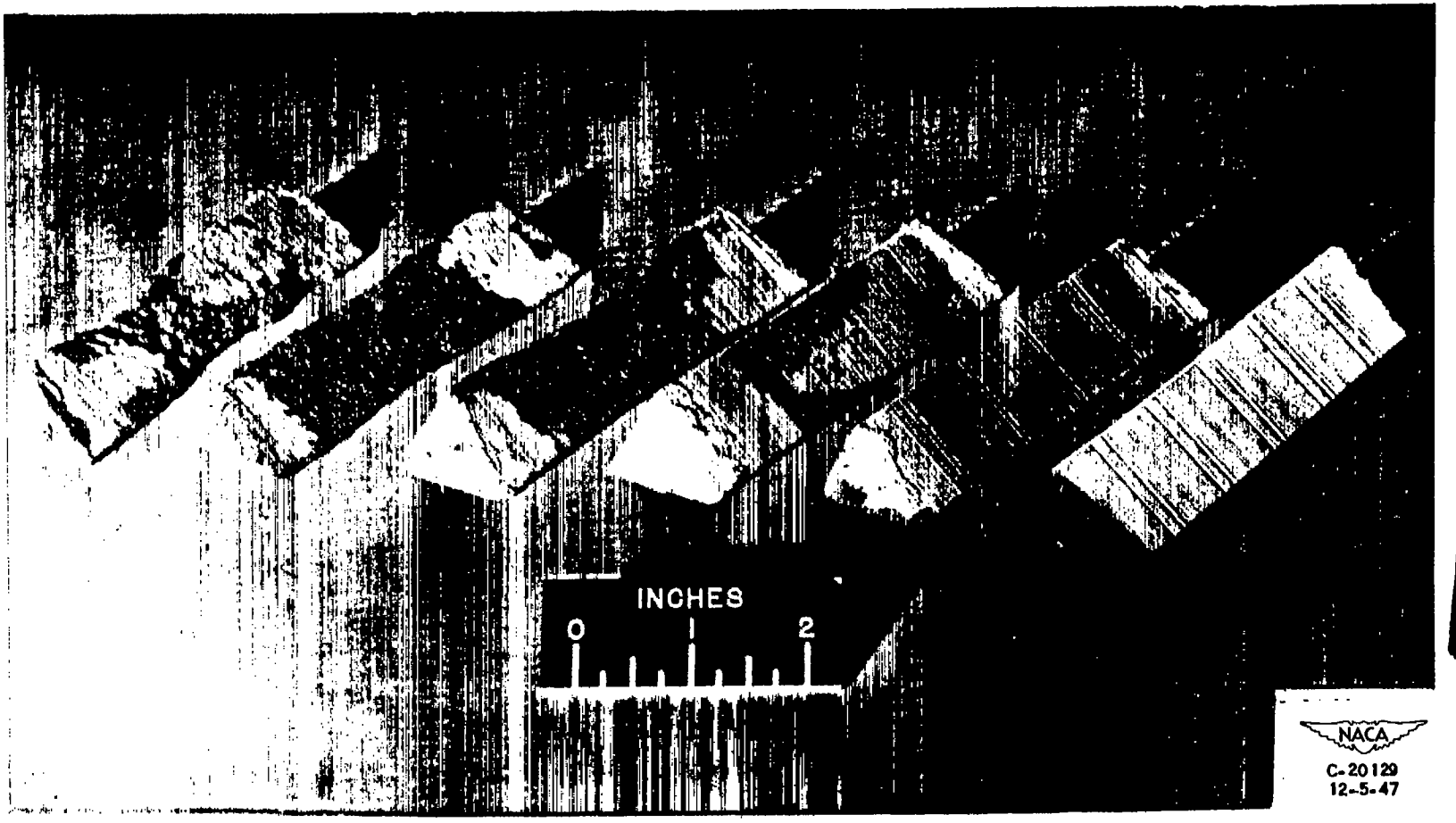

Figure 14. - Graphite wedges (aluminum-coated) at various stages of deterioration.

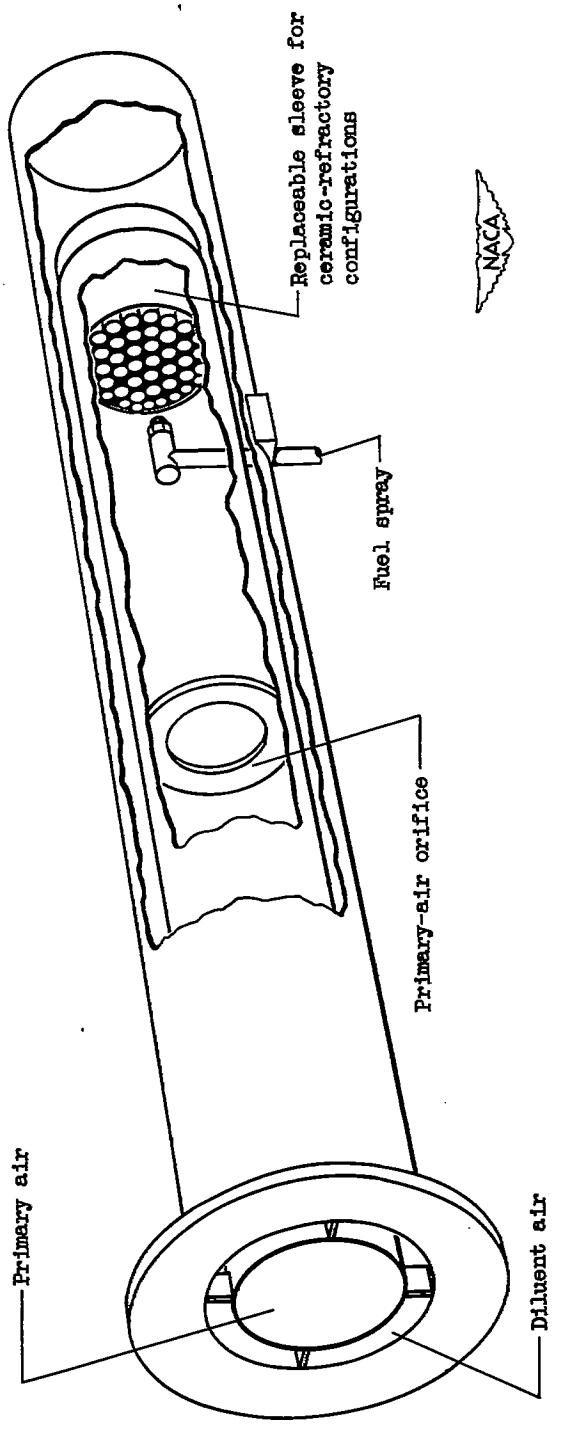

Figure 15. - Combustion chamber for ceramic-refractory study.

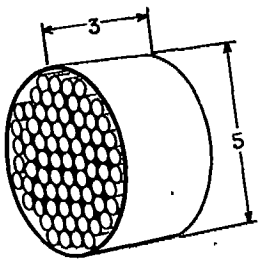

(a) Porous aluminum-oxide ceramic tubes. Inlet-air velocity, 50 feet per second; inlet-air pressure, 30 inches mercury absolute; combustion efficiency, 60 percent.

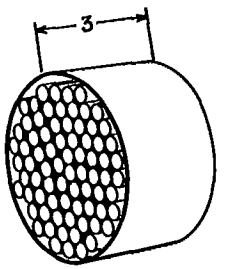

(b) Smooth impervious metallic-oxide ceramic tubes; unit failed to sustain combustion. Inlet-air pressure, 30 inches mercury absolute.

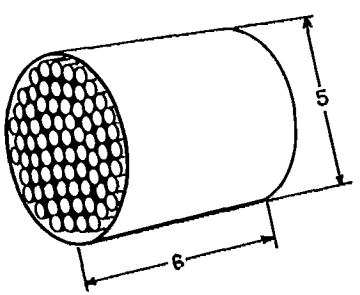

(c) Porous aluminum-oxide ceramic tubes. Inlet-air velocity, 100 feet per second; inlet-air pressure, 30 inches mercury absolute; combustion efficiency, 80 percent.

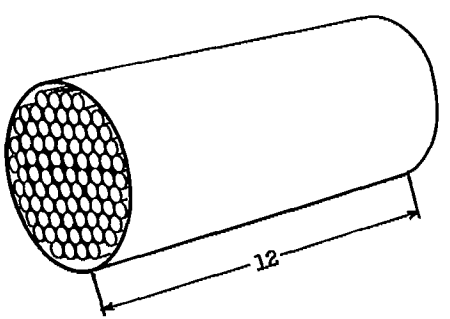

(d) Smooth impervious metallic-oxide ceramic tubes; unit failed to sustain combustion. Inlet-air pressure, 30 inches mercury absolute.

Figure 16. - Ceramic-refractory combustion-chamber configurations. Inlet-air temperature of 100° to 200° F and fuel-air ratio of 0.05 to 0.067. (All dimensions in inches.)

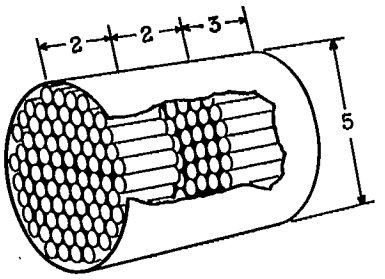

(e) Multiple-cluster chamber. First tube cluster, porous aluminum oxide; second tube cluster, smooth impervious ceramic. Inlet-air velocity, 74 feet per second; inlet-air pressure, 30 inches mercury absolute; combustion efficiency, 85 percent.

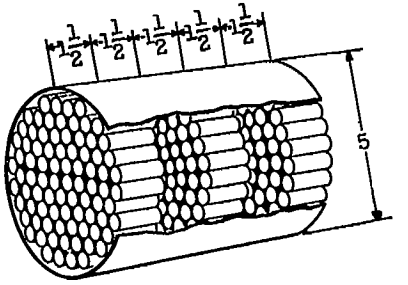

(f) Multiple-cluster chamber; three clusters composed of smooth impervious ceramic. Inlet-air velocity, 90 feet per second; inlet-air pressure, 30 inches mercury absolute.

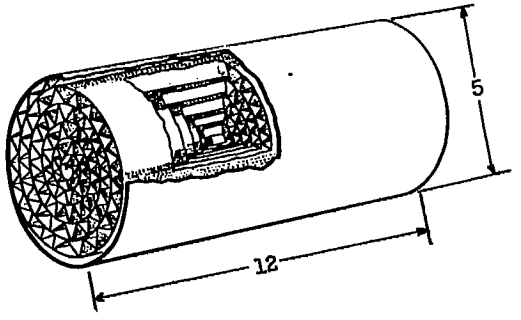

(g) Ceramic impregnated screen; unit failed in operation. Inlet-air pressure, 30 inches mercury absolute.

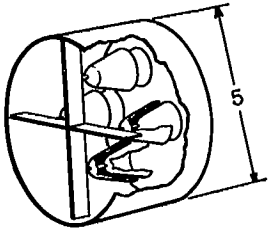

(h) Aluminum-oxide tandem cones. Inlet-air pressure, 30 inches mercury absolute.

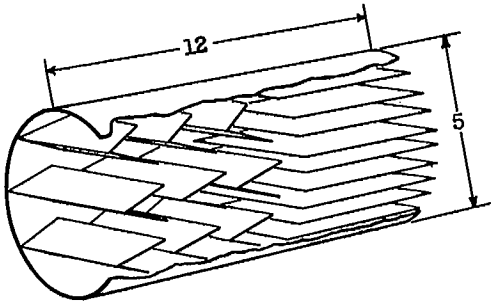

(i) Immersed gutter and gridwork composed of rhodium-plated tungsten sheet. Inlet-air velocity, 200 feet per second; inlet-air pressure, 55 inches mercury absolute; inlet-air temperature, 160° F; fuel, propane.

Figure 16. - Concluded. Ceramic-refractory combustion-chamber configurations. Inlet-air temperature of 100° to 200° F and fuel-air ratio of 0.05 to 0.067. (All dimensions in inches.)

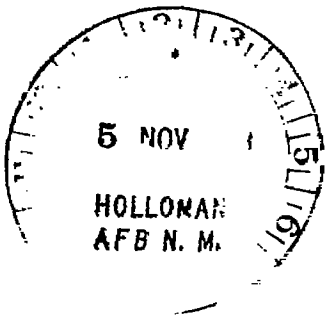
5 NOV
HOLLOMAN
AFB N. M.